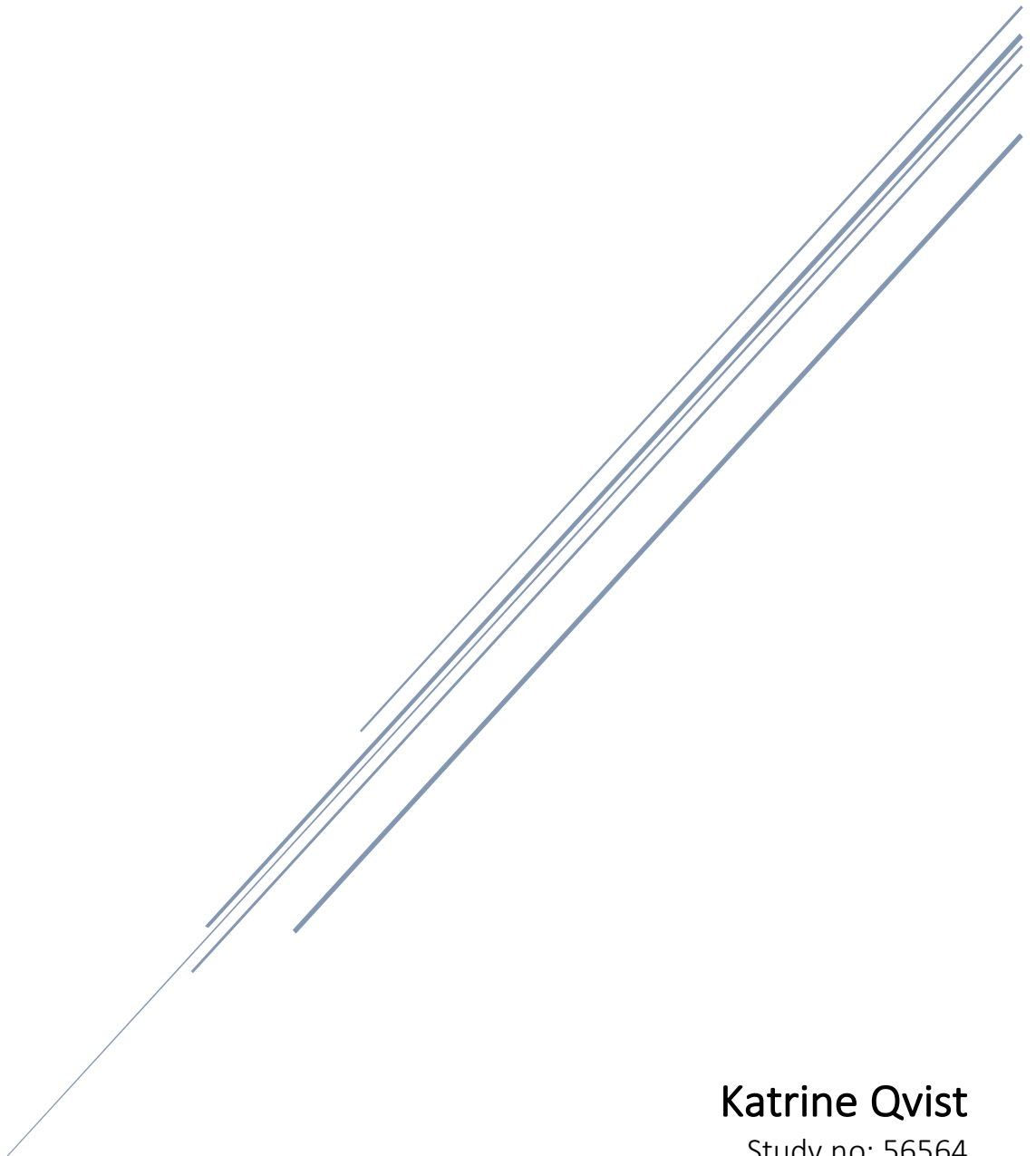


EFFECTS OF ANTIMICROBIAL PEPTIDES IN WOUND HEALING

60 ECTS - Roskilde University 2017-2018



Katrine Qvist

Study no: 56564



Preface

This work covers a 60-ECTS master thesis project in molecular and medicinal biology carried out at the department of science and environment at Roskilde University from August 2017 to June 2018.

Acknowledgments

I would like to thank my supervisor Professor Håvard Jenssen for his help and guidance throughout this thesis work. Also, I would like to acknowledge the help I've received in the lab from Kirsten Olesen, and other lab technicians at RUC, Thank you very much! Associate Professor Steen Seier Poulsen and his staff in the histology department at University of Copenhagen have let me use their lab and have helped with supervision and expert histological assessment, and for this they deserve a thank you as well. I have been lucky to share my office with a lot of fellow students who have been very helpful and always contributed with smiles, jokes and motivational pep-talks. PhD-students in the Jenssen group have also been helpful and supportive, and my friends and family all deserve thanks too, for putting up with my horrible science jokes and the general stress level I have experienced in the final months of this work.

Abstract

Diabetes and many of its subsequent complications like diabetic foot ulcer (DFU) is a serious problem world-wide. It has substantial consequences of both health and economy in many low- and middle-income countries and the rise of several antibiotic-resistant bacterial strains is intensifying the problem of treatment of these chronic and often infected wounds.

The aim of this thesis was to investigate wound healing properties of four antimicrobial peptides (AMPs) in the search for alternatives to antibiotic treatment of DFU. The four tested AMPs included two neuropeptides; neurotensin (NT) and substance P (SP), a known antimicrobial bacteriocin; nisin A, and a synthetically produced AMP; GN-2. Different assays were applied to assess immunomodulating and biofilm eradicating properties of the four AMPs. Static biofilm eradication assays were performed on single- and multispecies biofilms of *E. coli*, *S. aureus* and *S. epidermidis*. Biofilm eradicating effects of GN-2 and nisin A was determined by crystal violet staining for total biomass and PMA qPCR for viable cell counts. Furthermore, wound healing properties of all four AMPs were assessed by an *ex-vivo* porcine skin wound healing model.

Results confirmed some antimicrobial effects of GN-2 and better effects of nisin A but also demonstrated the vast difference between concentrations of antibiotic agents needed for killing of planktonic bacteria compared to biofilms. GN-2 and nisin A showed some wound healing effects at day one but no difference from control wounds on day three. The opposite effect was observed for SP, and especially for NT, with an increase of proliferating cells at day three but no difference from the control at day one.

In conclusion, different interesting effects on wound healing was observed by the four investigated AMPs adding to the elucidation needed for potential use of AMPs as therapeutic agents.

Resumé

Diabetes og mange af de efterfølgende komplikationer som diabetisk fodsår (DFU) er et alvorligt problem på verdensplan. Det har betydelige konsekvenser for både sundhed og økonomi i mange lav- og mellemindkomstlande, og identifikation af flere og flere antibiotikaresistente bakteriestammer øger problemet med behandling af disse kroniske og ofte inficerede sår.

Formålet med denne afhandling var at undersøge sårhelingssegenskaber for fire antimikrobielle peptider (AMPer) i søgen efter alternativer til antibiotika i behandlingen af DFU. De fire testede AMPer omfattede to neuropeptider; neurotensin (NT) og substance P (SP), et kendt antimikrobielt bakteriocin; nisin A og et syntetisk fremstillet AMP; GN-2. Forskellige analyser blev anvendt til vurdering af immunomodulerende og biofilmudryddende egenskaber hos de fire AMPer. Statiske assays for biofilmelimination blev udført på enkelt- og multispecies biofilm af *E. coli*, *S. aureus* og *S. epidermidis*. Biofilm-eliminerende effekt af GN-2 og nisin A blev bestemt ved krystalviolet farvning for total biomasse og PMA qPCR for tælling af levedygtige celler. Endvidere blev sårhelingssegenskaber af alle fire AMPer vurderet ved hjælp af en *ex-vivo* sårhelingsmodel på grisehud.

Resultaterne bekræftede nogen biofilm-eliminerende effekt af GN-2 og endnu bedre effekt af nisin A, men viste også den store koncentrationsforskel nødvendig for elimination af planktoniske bakterier contra udryddelse af biofilm. GN-2 og nisin A viste nogle sårhelings effekter på dag et, men ingen forskel fra kontrolsår på dag tre. Den modsatte virkning blev observeret for SP og især for NT med en forøgelse af prolifererende celler på dag tre, men ingen forskel fra kontrollen på dag et.

Som konklusion blev forskellige interessante virkninger på sårhelning observeret af de fire undersøgte AMPer, hvilket hjælper i den nødvendige klarlægning af AMPer, før en potentiel terapeutisk anvendelse af disse kan anbefales.

Preface	2
Acknowledgments	2
Abstract	3
Resumé	4
Introduction	7
Background	8
Human skin and wound healing	8
Diabetes and wound healing	9
Porcine skin as a model system for human wound healing	9
Bacterial infections	10
Biofilm	10
Multispecies biofilm	11
Antibiotics	12
Vancomycin	13
Ceftazidime.....	14
Rifampin	15
Antimicrobial Peptides	16
Nisin A.....	16
Substance P (SP)	17
Neurotensin (NT)	17
GN-2.....	18
Materials and methods	19
Strains and growth media	19
Biofilm eradication assay	19
Staining with crystal violet	20
PMA-qPCR quantification	20
Ex-vivo pig skin wound healing model	21
Immunohistochemical staining	22
Statistical analysis	23
Results	24

Biofilm eradication assay	24
Biofilm eradication – Total biomass measured by crystal violet staining	26
Biofilm eradication – Bacterial count determined by PMA qPCR	28
Standard curves	31
Wound healing	35
Discussion	44
Biofilm eradicating effects of AMPs	44
GN-2.....	45
Nisin A.....	46
Slow growing bacteria in biofilm	47
Method optimisation – Biofilm eradication assay	48
Biofilm eradication measured by crystal violet staining.....	48
Biofilm eradication determined by PMA qPCR.....	49
DNA-extraction	49
PMA treatment.....	49
qPCR	50
Wound healing properties of AMPs	51
GN-2.....	51
Nisin A.....	52
Substance P	52
Neurotensin.....	53
Method optimisation - Wound healing	55
AMPs as therapeutic agents	56
Conclusion	57
References	58
Appendix	64

Introduction

Diabetes is a serious health problem across the world today and studies predicts that incidents will only increase in the following years. Not only is it a health problem to those who suffer from the disease, it has also become a great economic burden for countries all over the world. Two thirds of people with diabetes live in low and middle income countries and estimates suggest that only one out of two with the disease has been diagnosed. A common complication of diabetes is chronic lower limb ulcers, so called diabetic foot ulcer (DFU). These chronic ulcers can lead to osteomyelitis, minor or major amputations and death if not treated. Global prevalence of DFU averages at the seemingly small number of 6,4% of diabetics, but in 2017 one third of diabetes costs were estimated to be linked to DFU¹.

DFU is a long-term complication of diabetes which is caused by a combination of several physiological imbalances where peripheral neuropathy and ischemia from peripheral arterial disease (PAD) are the main contributors. These circumstances, together with a trauma, can lead to chronic, and often infected, wounds which are hard to combat due to the poor wound healing capabilities of diabetic patients².

In chronic wounds like DFU bacterial infections will most often consist of sessile bacteria grouped together in a slimy matrix called biofilm. The tight structure of biofilms make treatment with conventional antibiotics difficult since most antibiotics needs to be in close proximity to bacteria to exert their antimicrobial effects, and many antibiotics cannot penetrate biofilms³. Because of these resilient biofilms, and since increasing numbers of bacteria develop resistance towards our conventional antibiotics, the need for other antimicrobial agents is rising. This is where antimicrobial peptides (AMPs) known for their antimicrobial and in some cases also immunomodulating abilities may have yet unnoticed application potentials⁴.

The aim of this study was to investigate antimicrobial and immunomodulatory effects of a number of selected AMPs. AMPs of both natural and synthetic origin were evaluated on their ability to eradicate single- and multi-species biofilms and their effect on wound healing in an *ex-vivo* porcine skin wound healing model.

Background

Human skin and wound healing

Human skin consists of multiple layers of different cell types. It has many functions including physical protection, regulation of body temperature, secretion, sensation and immune defence. The outer layer, epidermis, consists mostly of keratinocytes that move upwards as they mature. As they complete their lifecycle they shed off from the outer layer of the epidermis, stratum corneum. Beneath the epidermis lies the dermis, and beneath this is subcutaneous fatty tissue. Besides keratinocytes there are other cell types like melanocytes, Merkel cells and dendritic cells, and also accessory structures like hair follicles, sweat glands, and nerve fibres are found in the skin of humans.⁵

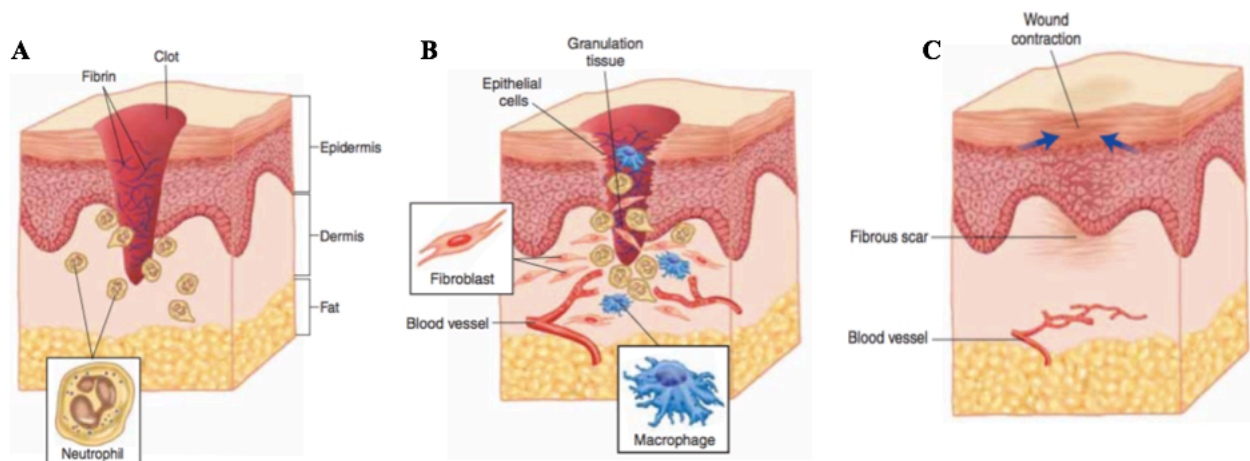


Figure 1 Composition of human skin and the three phases of wound healing. A: inflammation B: Proliferation C: Tissue remodelling. Picture adapted from⁶

The protective shield, which the skin constitutes, protects the organism from harmful substances like pathogens and physical stress from our surroundings. If this barrier is broken, for example by injury, surgery, infections etc., it can give rise to a wound. When this happens the carefully orchestrated mechanism of wound healing is crucial to restore and maintain the function of the skin barrier. Wound healing is a well-regulated but complex process that involves phases of inflammation, proliferation, and tissue remodelling⁷. The inflammatory phase begins at the time of injury. Neutrophils, macrophages and other leucocytes are attracted to ingest and remove bacteria. They also attract other cells important for the next phase of wound healing by production of cytokines. After 24-48 hours the proliferation phase begins where fibroblasts produce new skin cell components and growth factors needed for cell proliferation and angiogenesis. Epithelialization also starts around here with epithelial

cells at the wound edges proliferating and migrating inwards to form a new surface epithelial layer. The remodeling phase begins after approximately 3 weeks. The remodeling of skin cells and collagen synthesis results in a fibrous scar⁶.

Diabetes and wound healing

Under circumstances where one or more of the above-mentioned processes are compromised, the wound healing will be inefficient to restore the barrier function of the skin and the wound can become chronic. Diabetes can cause these circumstances as an effect of neuropathy and PAD with impaired angiogenesis and chronic inflammation favouring the establishment of a chronic and most often infected wound. Neuropathy or PAD will not result in ulceration alone, but the combination of these factors together with trauma can give rise to a wound. This wound might not be perceived by the patient due to the loss of sensation and might further be complicated by infection which is poorly combated by the immune system due to PAD². One of the key issues in the poor wound healing abilities of diabetics is the lack of blood flow to the wound area due to PAD. Blood supplies nutrients, inflammatory cells and oxygen to the wound area, which are all important components needed to establish conditions that favour host defence rather than bacterial growth⁸.

Porcine skin as a model system for human wound healing

To assess wound healing properties of the selected AMPs a model of human wounds was needed. Human skin however, is not an easily accessed research material. This is both because it is not often available in large quantities and because it can be associated with administrative impediments using human skin for research. In this case geographical limitations were also considered as transport times needed to be kept at a minimum to maintain cell viability in the skin. In Roskilde there is an education centre for the food manufacturing industry that was able to supply us with pig's ears, which is a by-product of their daily educational production. In the biomedical field of research the pig is considered an excellent model animal⁹ and especially when working with skin pigs are much more comparable to humans than "loose-skinned" animals like mice and rats who are otherwise commonly used in research. Comparisons between human skin and porcine skin has been investigated in regard to many different parameters; immunology¹⁰, histology¹¹, mechanical comparisons¹², and transdermal absorption of substances¹³.

Bacterial infections

Chronic wounds can hold many different bacteria and DFU is no exception. Polymicrobial infections are often seen in DFU and amongst the most frequently found Gram-positive bacteria are *Staphylococcus aureus*, *Staphylococcus epidermidis* and *Streptococcus pneumoniae*. The most commonly isolated Gram-negative bacteria are *Proteus spp.*, *Enterobacter spp.*, followed by *Escherichia coli*, and *Pseudomonas spp.*¹⁴ Chronic wounds and impaired wound healing will often mean infected wounds, and bacterial infections in chronic wounds are often dominated by biofilmproducing bacteria which can make treatment more difficult compared to treatment of planktonic bacteria. In this study we wanted to investigate the antimicrobial effects of AMPs on biofilm. For this, we selected both Gram-positive bacteria in *S. aureus* and *S. epidermidis* and a Gram-negative bacterium in *E. coli* **Table 1**. Both single species and multi species biofilms were applied.

Table 1 Bacterial strains

Bacteria name	Strain
<i>E. coli</i>	K12
<i>S. aureus</i>	Unknown (from KU)
<i>S. epidermidis</i>	ET-024 (methicillin resistant)

Biofilm

Biofilm has become subject of much scientific study since its discovery in the late 1970's where J. W. Costerton described the bacterial biofilm for the first time¹⁵. However, biofilms had already been described almost 300 years earlier. Antoni Van Leeuwenhoek described a form of bacteria within the plaque on teeth that were much more resilient than the bacteria outside the plaque¹⁶. This ability to tolerate high concentrations of antimicrobial substances

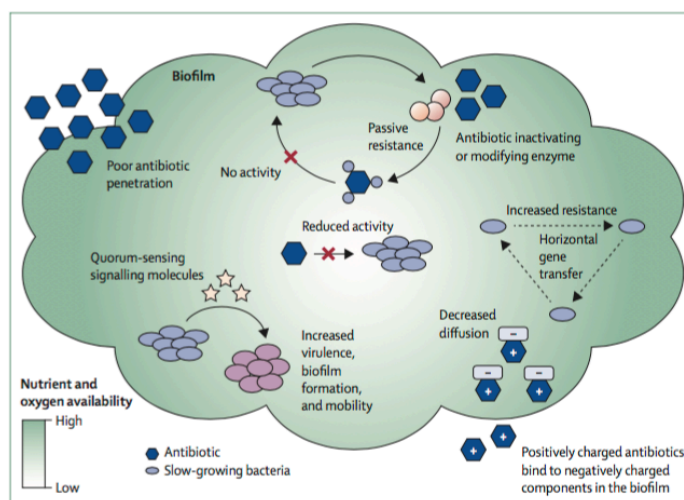


Figure 2 Structure of a biofilm and mechanisms of antibiotic tolerance⁸⁴

is a key property of the aggregate of bacteria that constitute a biofilm. Bacteria form physical bonds in this aggregate which binds them closely together. Furthermore, the bacteria produce an

extracellular matrix consisting of different types of extracellular polymeric substances (EPS) like proteins, polysaccharides and DNA. **Figure 2** illustrates the structure of a biofilm and show some of the traits that make biofilms resilient and able to withstand concentrations of antibiotics that would otherwise kill their planktonic equivalents³. Biofilm is formed on many surfaces and from our everyday life we recognize them e.g. as the slimy surface on the tiles of our bathroom or the plaque on our teeth as van Leeuwenhoek described it back in 1684. Not all bacteria form biofilm naturally but it is a defence mechanism utilised by many bacteria including variants of the three bacteria studied in this thesis; *E. coli*, *S. aureus* and *S. epidermidis*.^{17,18}

Multispecies biofilm

A lot of research has been made on biofilm from different single species bacteria but wounds like DFU and most other biofilms in nature will often consist of multiple species of bacteria. These different bacteria can interact in countless ways determining the structure and fitness of a multispecies community like a biofilm. First of all, different species will organize in different ways and interactions between species can either be cooperative, competitive or exploiting. An illustration of different interspecies interactions is pictured in figure 3. Secondly, bacteria inside a multispecies biofilm will interrelate both by cell-cell and cell-environment interactions. Examples of both co-metabolism and competitive metabolism are seen and there are even examples of non-biofilm forming species that will form biofilm only in the presence of other species. The high tolerance towards antimicrobial substances that biofilms can exert is an effect of all these different factors together. It depends on special structure, interactions amongst bacteria, amount of ESP and of course also place and age of the biofilm and the chemical composition of the environment.¹⁹

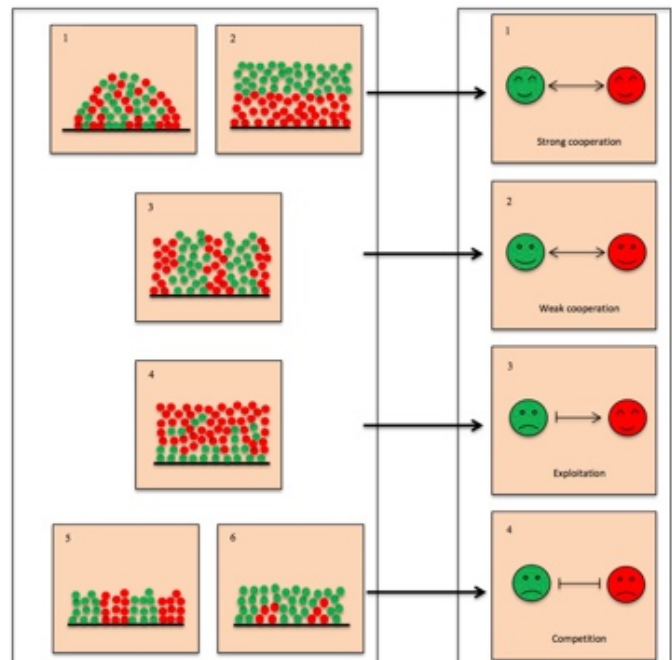


Figure 3 Spatial organization and interactions in multispecies biofilms¹⁹

Antibiotics

The introduction of the antibiotic era in the early 1900's has been a landmark in healthcare all over the world, most notably stated by the introduction of Salvarsan in 1910²⁰ a treatment against syphilis, and its replacement penicillin in the early 1940's²¹. Unfortunately, the invention of new antibiotics is not keeping up with the emergence of resistance towards the conventional antibiotics we use today. Actually there has been a long period without development of new classes of antibiotics from the early 1960's to 2000²². Several reasons for this decline in new antibiotics have been suggested. The most supported of these are the financial aspect. It seems more financially favourable to aim for development of medicine for chronic diseases than for antibiotics which are used for a much shorter time period. Also, some researchers suggest that the source of naturally derived antibiotics is simply exhausted²³.

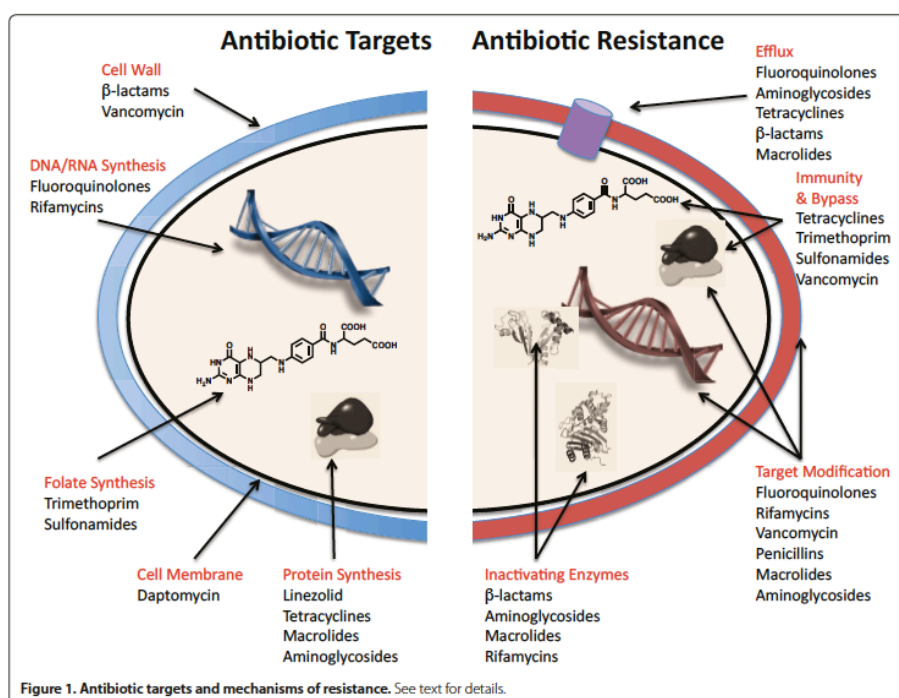


Figure 4 Antibiotic targets and mechanisms of resistance²³

Antibiotics are most often grouped by their microbial target. There are 5 major targets; The bacterial cell wall, the cell membrane, protein synthesis, DNA and RNA synthesis, and folic acid metabolism illustrated in Figure 5. Three conventional antibiotics, which inhibits cell wall synthesis or DNA/RNA synthesis, are included in this thesis and the mechanism of these three antibiotics will be described in the following. As mentioned earlier antibiotic resistance is becoming an increasing problem. There are different ways that microorganisms can acquire resistance and these are also visualized in Figure 5. The strain of *S. epidermidis* ET-024 is methicillin-resistant which will be

discussed later, but otherwise none of the selected bacteria are resistant to antibiotics. All three antibiotics are listed on WHO's Model List of Essential Medicines, which contains the medications considered to be most effective and safe to meet the most important needs in a healthcare system²⁴.

Vancomycin

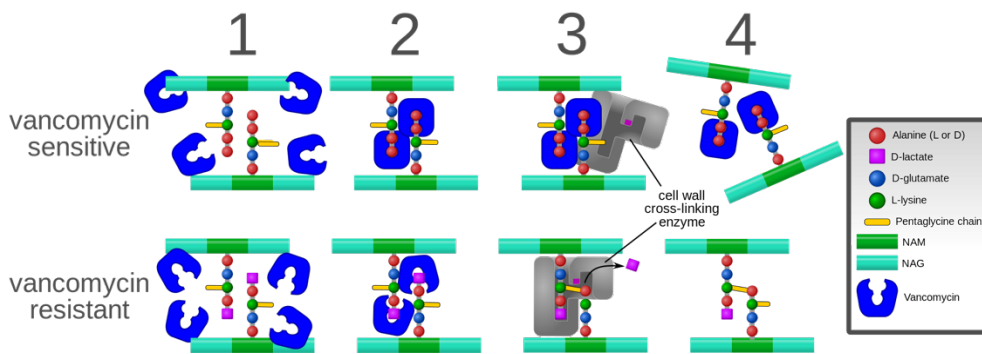


Figure 5 Mechanisms of vancomycin action and resistance⁸³

Vancomycin is a bactericidal glycopeptide derived from the actinobacteria *Amycolatopsis orientalis*. It is part of the group that has the bacterial cell wall as its target. Vancomycin inhibits the cell wall synthesis by preventing cross-linkage of the peptidoglycan units that comprises the cell envelope. An intact cell wall is crucial for the survival of a bacteria as it constitutes protection against alternating environmental conditions like osmotic pressure and hazardous components. The cell wall is constantly maintained by adding and cross-linking new peptidoglycan constituents and this process is catalyzed by transpeptidase and transglycosylase. Vancomycin inhibits the synthesis of the peptidoglycan layer by binding to peptidoglycan units and by blocking transpeptidase and transglycosylase²⁵. Vancomycin is not able to penetrate the cell wall of Gram-negative bacteria but is effective against Gram-positive bacteria like staphylococci. It was usually reserved for serious Gram-positive bacterial infections and for bacterial endocarditis and resistance to vancomycin was uncommon only 10-20 years ago.²⁶ Today however, an increasing number of vancomycin resistant *S. aureus* are reported.²⁷

Ceftazidime

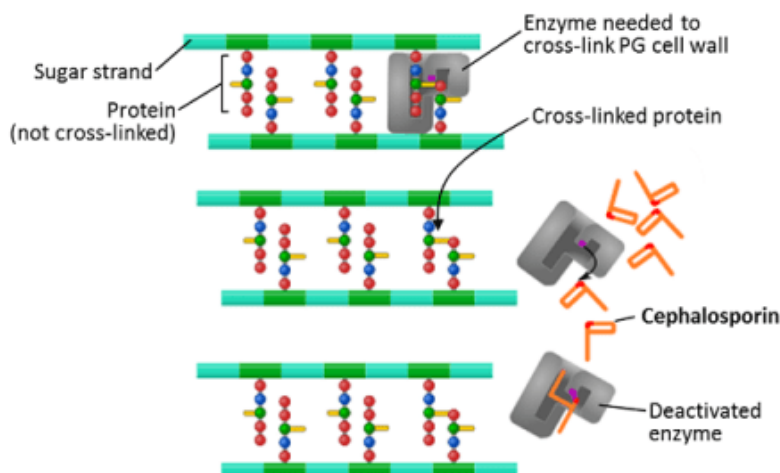


Figure 6 Mechanism of chephalosporins²⁸

Ceftazidime is a cephalosporin included in the β -lactam family of antibiotics which also includes penicillins and carbapenems. They are named after the β -lactam ring they all have that needs to be intact for them to be active. Cephalosporins are semisynthetic antibiotics. The parent compound, cephalosporin C, was first derived from the bacterium *Cephalosporium acremonium*. This compound has since been adapted by addition of side chains making the antimicrobial activity of the compound greater²⁹. Different generations of cephalosporins exists and ceftazidime is part of the third generation, which are more stable against β -lactamase inactivation compared to the earlier generations. This generation of cephalosporins has increased activity against Gram-negative bacteria but only low activity against Gram-positive²⁶. Ceftazidime also has the bacterial cell wall as its antibiotic target. Much like vancomycin it blocks the cross-linkage of peptidoglycan units by inhibiting the peptide bond formation which is catalysed by transpeptidase enzymes²⁵.

Rifampin

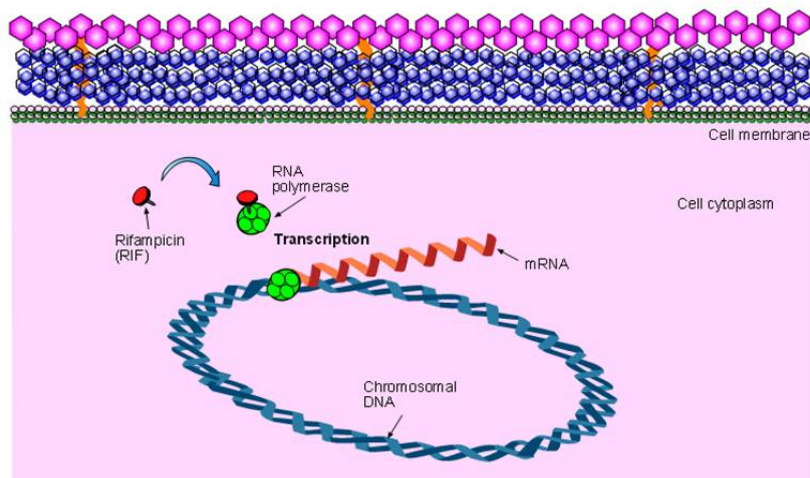


Figure 7 Rifampin mechanism³⁰

Rifampin is a semisynthetic derivative of rifamycin – a fermentation product of the bacteria *Nocardia mediterranea*. Rifampin has the DNA-dependent mRNA transcription as its antibiotic target. Rifampin inactivates the RNA-polymerase that catalyses the transcription of mRNA from DNA which results in a bactericidal effect³¹. Rifampin has a broad spectrum of activity against mycobacterial infections like *Mycobacterium tuberculosis*, legionella infections and serious staphylococcal infections and endocarditis. Most often it is used in combination with other classes of antibiotics to prevent resistance which develops rapidly for rifampin²⁶.

Table 2 Minimal inhibitory concentrations of antibiotics

	<i>E. coli</i>	<i>S. aureus</i>	<i>S. epidermidis</i>
Vancomycin		0,5-2 µg/ml	0,5-4 µg/ml
Ceftazidime	0,064-0,5 µg/ml		
Rifampin		0,004-0,032 µg/ml	0,004-0,064 µg/ml

MIC values from EUCAST database³²

Table 3 Minimal inhibitory concentrations of AMPs

	<i>E. coli</i>	<i>S. aureus</i>	<i>S. epidermidis</i>
Nisin A		1,5-83,6 µg/ml ³³	4,19 µg/ml
GN-2	16 µg/ml ³⁴	8 µg/ml ³⁴	

Antimicrobial Peptides

Peptides are smaller proteins consisting of up to 50 amino acids. Peptides are found as part of innate defence mechanisms to protect against potentially harmful pathogens in both prokaryotes and eukaryotes. Peptides that can kill or inhibit microorganisms are called antimicrobial peptides (AMPs) and due to the role of some naturally found AMPs in the innate immune defence these are also called host defence peptides.

AMPs vary in size, composition, cytotoxicity and mode of action but most are cationic amphipathic peptides that can bind to and kill or inhibit microorganisms like Gram-positive and Gram-negative bacteria, fungi, yeast, protozoa and viruses³⁵.

Bacteria themselves produce AMPs too. They help them communicate amongst each other and suppress other bacteria in a competitive environment – these AMPs are called bacteriocins³⁶. Since the scientific interest in AMPs have increased and the possibility of utilising these as antimicrobial agents, the search for new peptides have intensified and have even surpassed isolation of peptides from natural sources like defensins and bacteriocins. Both modification of natural AMPs and the de novo design of synthetic AMPs have led to numerous new AMPs to be tested and unquestionably more will follow³⁷. The peptides used in this work has been selected because of their proved antimicrobial effects on a variety of bacteria, but also based on their potentially immunomodulating effects which may have effect on wound healing.

Nisin A

Nisin A is a bacteriocin - an antimicrobial peptide which is naturally produced by the bacteria *Lactococcus lactis*. nisin has been utilized in the food industry as a preservative due to its antimicrobial properties for several years. Nisin is an elongated cationic polypeptide, consisting of 34 amino acids including some more unusual amino acids like 3-methylanthionine and lanthionine. Hence, it is a member of the lantibiotics – i. e. *lanthionine* containing *antibiotics*. Due to its composition and a unique structural modification, nisin A is able to exert its bactericidal effect on other mostly Gram-positive bacteria. It does so primarily by membrane perturbation. A high stability and the pleiotropic activity of lantibiotics might very well be part of the reason that other bacteria are limited in gaining resistance against them.^{36,38}

This limitation of resistance development and the fact that nisin A has very low toxicity makes it interesting as a potential antimicrobial agent to combat infectious disease in the medical field. Nisin A, along with other Type I lantibiotics, have been studied and shown to not only be effective against

methicillin-resistant *S. aureus* (MRSA)³⁶ but also have immunomodulating abilities³⁹ as well as wound healing properties^{40,41}.

Substance P (SP)

Substance P (SP) is a neuropeptide. Just like bacteria and other animal cells use molecules to communicate, neurons use neuropeptides to communicate and to exert effects on surrounding cells. SP is widely distributed in the brain and in the peripheral nervous system and also in many peripheral tissues. SP binds to its receptors; neurokinin (NK)-1, -2, and -3 where NK-1 is the predominant receptor. NK-1 is found on immune cells, endothelial cells, epithelial cells etc. At the site of an injury SP is released and it will take part in the initial phase of wound healing; inflammation. SP will attract leukocytes and other immune cells as well as stimulate vasodilation and epithelial adherence⁴². SP is present in dermis and epidermis and it has been shown to stimulate angiogenesis as well as proliferation of both fibroblasts and keratinocytes, which suggests that SP is associated with not only inflammatory response but also could have effect on the proliferation and remodelling phases of wound healing^{43,44}. SP is metabolized by an enzyme called neutral endopeptidase (NEP). It has been shown that NEP expression is elevated in skin of diabetics and thereby reducing amounts of SP⁴⁵. All things considered, it is speculated that SP can have an effect on wound healing both in regular uninfected wounds and in chronic infected wounds characterized in DFU.

Neurotensin (NT)

Like Substance P, neurotensin (NT) is another neuropeptide. NT is found most abundantly in the brain and endocrine cells of the gut but it is also found in other peripheral tissues like the skin. Here, it has chemotactic effects on immune cells like leukocytes, mast cells, and macrophages which are all important participants in the orchestration of a correct immunomodulating response. Also, fibroblasts and keratinocytes are affected. NT exerts its effect by binding to specific receptors called NT-receptor (NTR) -1, -2 and -3 where NTR1 is the most abundant receptor with highest affinity. NT has also been shown to affect vessel permeability, vasodilation/vasocontraction and improve angiogenesis which is one of the important wound healing mechanisms impaired in diabetics.^{42,46}

Since NT is more abundant in the gut and CNS more research has been made in these areas but some research has been made in the application of NT on skin cells and in wounds.^{46,47} These studies show that NT can affect a pro-inflammatory status in both macrophages and dendritic cells and one study

has also shown a direct effect on wound size after application with NT in an in vivo wound healing model⁴⁶.

GN-2

Since AMPs have reached great scientific interest as a possible source of novel antibacterial agents, more ways of producing peptides have come up. Where the other peptides used in this work are derived from either humans or bacteria, the GN-2 peptide is a synthetically produced peptide. It is one out of a cohort of peptides generated through a QSAR- based *in silico* approach, where software was used to very specifically predict highly active AMPs³⁴.

GN-2 is a 9 amino acid peptide with the same characteristic features as most other active AMPs; positive net charge, amphipathic structure and associated with bacterial membrane permeabilization³⁷.

Table 4 Sequence, origin and overall charge of different antimicrobial peptides

	Amino acid sequence	Origin	Charge
GN-2	RWKRWWRWI-CONH ₂	Synthetic	+4
Nisin A	ITSISLCTPGCKTGALMGCNMKTATCHCSIHVSK	Bacteria	+3
Neurotensin	QLYENKPRRPYIL	Human	+2
Substance P	RPKPQQFFGLM	Human	+3

Materials and methods

Some of the methods used in this thesis was subject for a great deal of adjustments and trial and error before ending up with the techniques listed below. Especially the pig skin model was completely new territory so quite a lot of time has been used to try and perfect this method. Very little literature and sparse descriptions of the wounding process and applied instruments, let to different designs and techniques to be tested. Pictures of the different tested instruments are found in **Figure 30** in Appendix.

Strains and growth media

Bacterial strains were obtained from in house strains of *Escherichia coli* (*E. coli*), *Staphylococcus aureus* (*S. aureus*) and *Staphylococcus epidermidis* (*S. epidermidis*). Bacteria were taken from -80°C and grown on LB agar plates ON at 37°C. For biofilm assays one colony was inoculated in 5 ml media and grown for 24 h at 37°C with shaking. Several different growth media were tested and Tryptic Soy Broth + 0,25 % glucose (TSB) was chosen as the best common growth media for all three bacteria. Repeated tests of the ON culturing method led to inoculums containing CFU/ml as listed here: *Escherichia coli*: 1,2–1,7*10⁻⁹, *Staphylococcus aureus*: 4,1-6,8*10⁻⁸, *Staphylococcus epidermidis*: 0,57-1,8*10⁻⁸.

It seems that the strain of *E. coli* we had available did not make a lot of biofilm on its own. We tried several different growth media where the bacteria were growing well in inoculums but wasn't able to produce a stainable biofilm in the 96 well plates. We chose to proceed with the *E. coli* strain because we wanted to investigate polymicrobial biofilms and did not want to settle for two staphylococci. We also wanted to test a Gram-negative bacterium and since *E. coli* is a common find in DFU we found it interesting to include this. We suspect that *E. coli* could still be involved in a multi-species biofilms when other strong biofilm making bacteria are present.

Biofilm eradication assay

Biofilm formation and staining with crystal violet were conducted according to the microtiter dish biofilm formation protocol⁴⁸ and described in short in the following.

Inoculums of each bacteria containing 10⁸-10⁹ CFU/ml were diluted 1:100 and 100 µl transferred to a flat-bottomed 96 well plate. The plate was incubated at 37°C for 4 h to allow the first bacteria to attach and make biofilm. During these 4 hours, the ON culture was left at room temperature to prevent continuing growth, and a new 1:100 dilution was made right before addition of the second bacteria.

The planktonic bacteria left after the four hours of incubation were removed and the second bacteria were added and allowed to develop biofilm overnight. On day two 100 µl of peptides or antibiotics, suspended in TSB, were added along with a non-treated control using TSB alone, and the plate was incubated overnight. All samples were made in triplicates and non-inoculated media controls were included.

Staining with crystal violet

After incubation with peptides or antibiotics the biofilm was washed twice in 150 µl PBS to remove planktonic bacteria. 125 µl of 0,1 % crystal violet was added and the plate was incubated at room temperature for 10 min. The crystal violet dye was removed using a multi-well pipette and the plate was gently submerged under two sets of demineralised water to remove all unbound colour. 200 µl of 99 % ethanol was added and mixed by pipetting vigorously up and down in each well to dissolve the colour bound by the biofilm formed on the bottom of the wells. 150 µl were transferred to a new flat-bottomed 96 well plate and OD₅₉₀ was measured on a spectrophotometer.

PMA-qPCR quantification

PMA-qPCR of biofilm was adapted from Luo et al.⁴⁹ with minor modifications.

After incubation with peptides or antibiotics the biofilms were washed twice in 150 µl PBS to remove planktonic bacteria. 100 µl of TSB was added to each well and mixed by vigorous pipetting to release biofilm from the bottom of the wells. 90 µl from each of the three replicate wells were transferred to one Eppendorf tube and 30 µl of PMA (2 mM) was added to a final volume of 300 µl. 10 min incubation at 37°C in the dark was followed by 15 min of photoactivation. For this step, Eppendorf tubes were placed on a carousel which mixes the samples while they get photoactivated by a 2400 Lumen LED lamp placed 20 cm from the samples. After photoactivation, where PMA has bound to DNA of compromised bacteria, the Eppendorf tubes were centrifuged shortly and supernatant was discarded. From the existing pellet, DNA was extracted using 500 µl TRI-reagent (T9424, Sigma Aldrich) according to manufacturer's protocol⁵⁰. Quantification of bacteria in each sample was made by qPCR (Lightcycler 96, Roche Diagnostics) with designed specific primers (Sigma Aldrich). Name and sequence of primers are listed in Table 5. For each reaction 1µl DNA was used together with 5 µl SYBR green, 1 µl of forward and reverse primer, and 2 µl of sterilised water. Results were calculated using standard curves made from DNA extractions from planktonic bacteria of known quantities.

Table 5 Names and sequences of primers used for qPCR

Primer name	Primer sequence
E. coli	Forward: AGAAGCTTGCTCTTTGCTGA Reverse: CTTTGGTCTTGCGACGTTAT
S. aur 149	Forward: ACTACATGAAGCTGGAATCGC Reverse: CCTTCGACGGCTAGCTCCTA
S. epi 193	Forward: CGGATAATACACCGTCATTCCAGACC Reverse: AGAACGTGCTAAAGAACAAGGCTA

Table 6 qPCR programme

Step	Time	Temperature
Preincubation	15 min	95°C
Amplification		
Denaturation	30 sec	95°C
Annealing	30 sec	65°C (62°C for E. coli)
Extension	30 sec	72°C
Melting		
	60 sec	95°C
	30 sec	55°C
	1 sec	95°C
Number of amplification cycles = 45		

***Ex-vivo* pig skin wound healing model**

The wound healing model in this work was developed with inspiration from the patented *ex-vivo* skin models DE10317400A1 and EP1927656A1. Pig's ears were supplied by the Education Centre for the Food Manufacturing Industry in Roskilde. Time used for transport and processing (on ice) was kept to a minimum – no more than 2 hours from the pig were slaughtered to skin samples, with inflicted wounds, were placed in growth media and incubated. Skin from the inner side of pig's ears was used. The bulky lines from the inside of the ear (plicae scaphae) are preferred due to the underlying layer of subcutaneous fat. Before wounding, the pig ear was washed in cold running water to get rid of dirt and blood. Hair was cut with scissors and the skin was sterilized with 70% ethanol. Wounds were made with a 2 mm diameter biopsy punch. A list with pictures of all the different wounding tools that were tested, before ending up with the biopsy punch, is found in **Figure 30** in Appendix. Preferably wounds should include only epidermis and a very small part of the upper dermis. After wounding, skin was cut from the cartilage of the ear so only epidermis, dermis and subcutis was conserved. Skin pieces of approximately 1x1 cm containing one wound were cut and rinsed, first in 70% ethanol and

then in PBS. Here, at time 0, one skin piece from each of the three replicates was preserved in 4% paraformaldehyde and the remaining skin pieces were placed on sterile gauze in 12 well plates. Approximately 1,5 ml of Dulbecco's Modified Eagle Medium (DMEM) pH 7.4, supplemented with 10% heat inactivated fetal bovine serum, 1% penicillin/streptomycin, without phenol red, containing 25 µg/ml peptide was poured over the skin piece so the wound was soaked and the well was filled to the point where subcutis and dermis were submerged but the skin surface and the wound was above the air-liquid interphase. Media with peptide was changed every 24 h. At day 1 and day 3 samples were preserved in 4% paraformaldehyde. Plates were incubated at 37°C in a humidified incubator with 5% CO₂ during the 3 days of the experiment.

Immunohistochemical staining

Skin samples were fixed in 4% paraformaldehyde for a minimum of 2 days. After fixation, samples were cut transversely through the wound and embedded in paraffin. Sections of 4 µm were cut on a microtome and put on electrostatically treated microscope slides and incubated at 60°C for 1 h to heat-fix sections and melt paraffin. Paraffin was removed by incubation in Tissue-clear (1466, Sakura) for 10 min and slides were hydrated through decreasing percentages of ethanol to water. Slides for Haematoxylin and Eosin staining (H&E) were stained following routine protocol (5 min in haematoxylin and 5 min in eosin). Slides for immunohistochemical staining were boiled for 15 min in T-EG buffer pH9 (10mM Tris-base + 0,05mM EGTA) to perform epitope retrieval. Non-specific antibody binding was blocked by incubation with 2% bovine serum albumin for 10 min. at room temperature. Samples were washed three times in PBS and incubated with primary antibody ki67 (1:1000, ab16667, Abcam) overnight at 4°C. After three washes in PBS samples were incubated with a biotin-conjugated secondary antibody (1:200, BA-1000, Vector laboratories) for 40 min at room temperature. Another wash cycle was applied and then samples were incubated with 3% hydrogen peroxide to block endogenous peroxidase activity. Amplification of the signal from the secondary antibody was achieved by 30 min incubation with a pre-formed avidin- and biotinylated horseradish peroxidase macromolecular complex (ABC) (PK-4000, Vector Laboratoris). To visualize the reactive area in the tissue samples were treated with 3,3-diaminobenzidine (DAB) (4170, Kem-En-Tek Diagnostics) for 15 min and 0,5% copper sulphate for 2 min. Finally, a brief counterstaining of cell nucleus in haematoxylin was applied before mounting of cover slides and assessment by light microscopy.

Statistical analysis

Data calculated from repeated values was analyzed using students t-test and unpaired one-way ANOVA in Graphpad Prism 7. Results are expressed as means + SD. *P* values less than 0,05 were considered statistical significant.

Results

This study aimed at identifying different wound healing properties of AMPs in the search for potential therapeutic applications. Antimicrobial activity was investigated for two AMPs and three conventional antibiotics by a microtiter dish biofilm eradication assay. Multi- and single-species biofilms of *E. coli*, *S. aureus* and *S. epidermidis* were applied. Following biofilm eradication assay total biomass was assessed by crystal violet staining and quantification of viable bacteria were assessed by PMA qPCR. Besides direct antimicrobial killing immunomodulating abilities of four AMPs were tested. This was investigated by an *ex-vivo* porcine skin wound healing model. Wounds were inflicted on porcine ear skin and treated with peptide for three days. Samples were taken on day 0, 1 and 3 to assess wound closure by epithelial migration.

Biofilm eradication assay

Antimicrobial effects of nisin A and GN-2 was investigated by biofilm eradication assays with single- and multi-species biofilms containing *E. coli*, *S. aureus* and *S. epidermidis*. Single- and multispecies biofilms were grown for 24 h and thereafter treated with different antimicrobial peptides for 24 h. Planktonic bacteria were removed, biofilms were stained with crystal violet, and OD₅₉₀ was measured. **Figure 8** and **Figure 9** illustrate different time points of the biofilm eradication assay which caused for concerns about reproducibility. Inconsistencies between replicate wells after different wash steps were macroscopically visible. It was evident that rather large amount of biofilm was removed by initial wash steps in **Figure 8** and removal of stained biofilm in an almost flaky manner after the final wash step is seen in **Figure 9**. Even though gained experience through multiple repeats of the assay helped, these inconsistencies resulted in substantial SD values of biofilm biomass measurements (**Figure 11** and **Figure 12**).

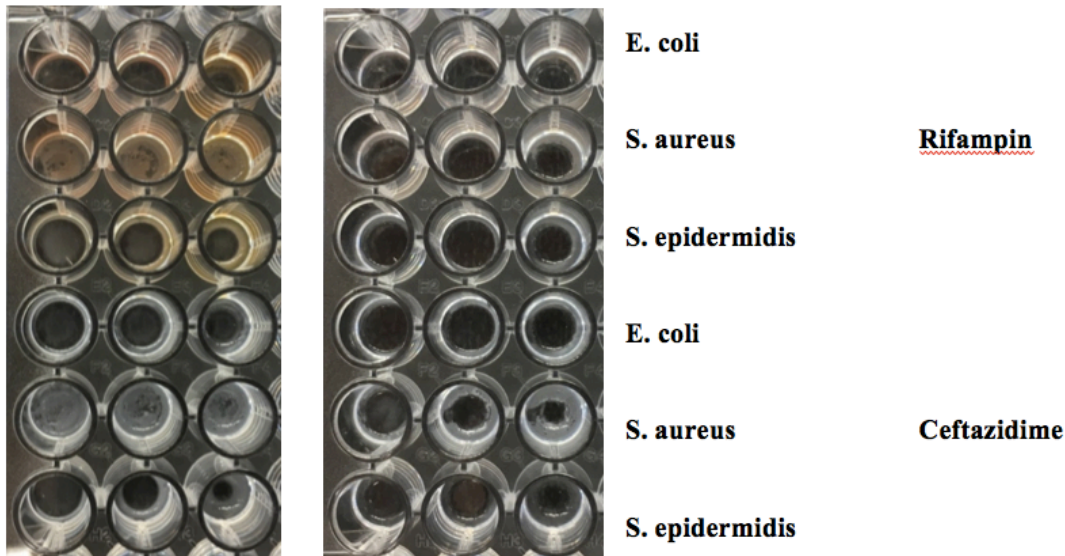


Figure 8 A: Wells with single-species biofilms after 24 h of treatment where media containing planktonic bacteria has just been removed (before wash) B: The same wells as A after two washes in 150 μ l of PBS. The three upper rows were treated with rifampin (300 μ g/ml), the three lower rows were treated with ceftazidime (300 μ g/ml). Every sample was made in triplicate (3 consecutive wells) and the assay was repeated three times.

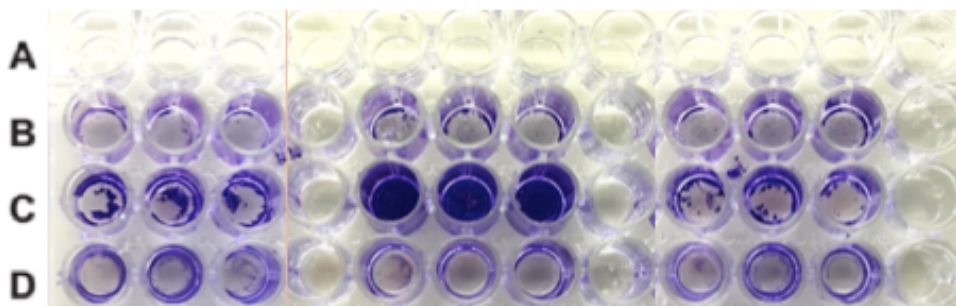


Figure 9 Wells with single- and multi-species biofilms after 24 h of vancomycin treatment (300 μ g/ml). Plate set-up is seen in figure 10. Biofilms were washed twice in PBS, stained with crystal violet for ten minutes, and washed by submerging the microtiter plate under tap water and draining twice. After this step, the remaining crystal violet dye bound to biofilm is solubilised by addition of 96% ethanol and OD₅₉₀ is measured. Every sample was made in triplicate (3 consecutive wells) and the assay was repeated three times.

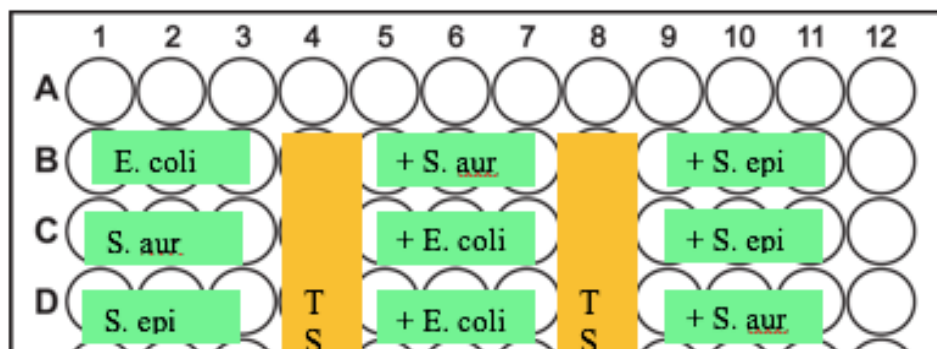


Figure 10 Plate set-up for the microtiter dish illustrated in Figure 9

Biofilm eradication – Total biomass measured by crystal violet staining

Following staining of biofilms total biofilm biomass was assessed by OD₅₉₀. Three conventional antibiotics were tested as controls along with GN-2 and nisin A. Results, illustrated in the figures below, clearly illustrates that biofilms are resilient as neither antibiotics nor AMPs were able to fully eradicate biofilms. Antibiotics showed no significant biofilm eradication on either of the single- or multi-species biofilm. Results in **Figure 11** might suggest a minor eradicating effect of rifampin on biofilms where *S. aureus* or *S. epidermidis* were seeded first (the two lower set of graphs), but this is a very modest effect. GN-2 and nisin A had greater biofilm eradicating effects than the antibiotics but none of the antimicrobial agents tested were able to completely eliminate biofilms. As large variations occurred, in the amount of biofilm produced by the different bacteria in this assay, some bars in the graphs in **Figure 11** have excessively high y-axis. Also, large amounts of data are plotted into these graphs. Therefore, some of the results were selected and illustrated as fold change in **Figure 12**, to get a better visualization of the biofilm eradicating effects of nisin A and GN-2.

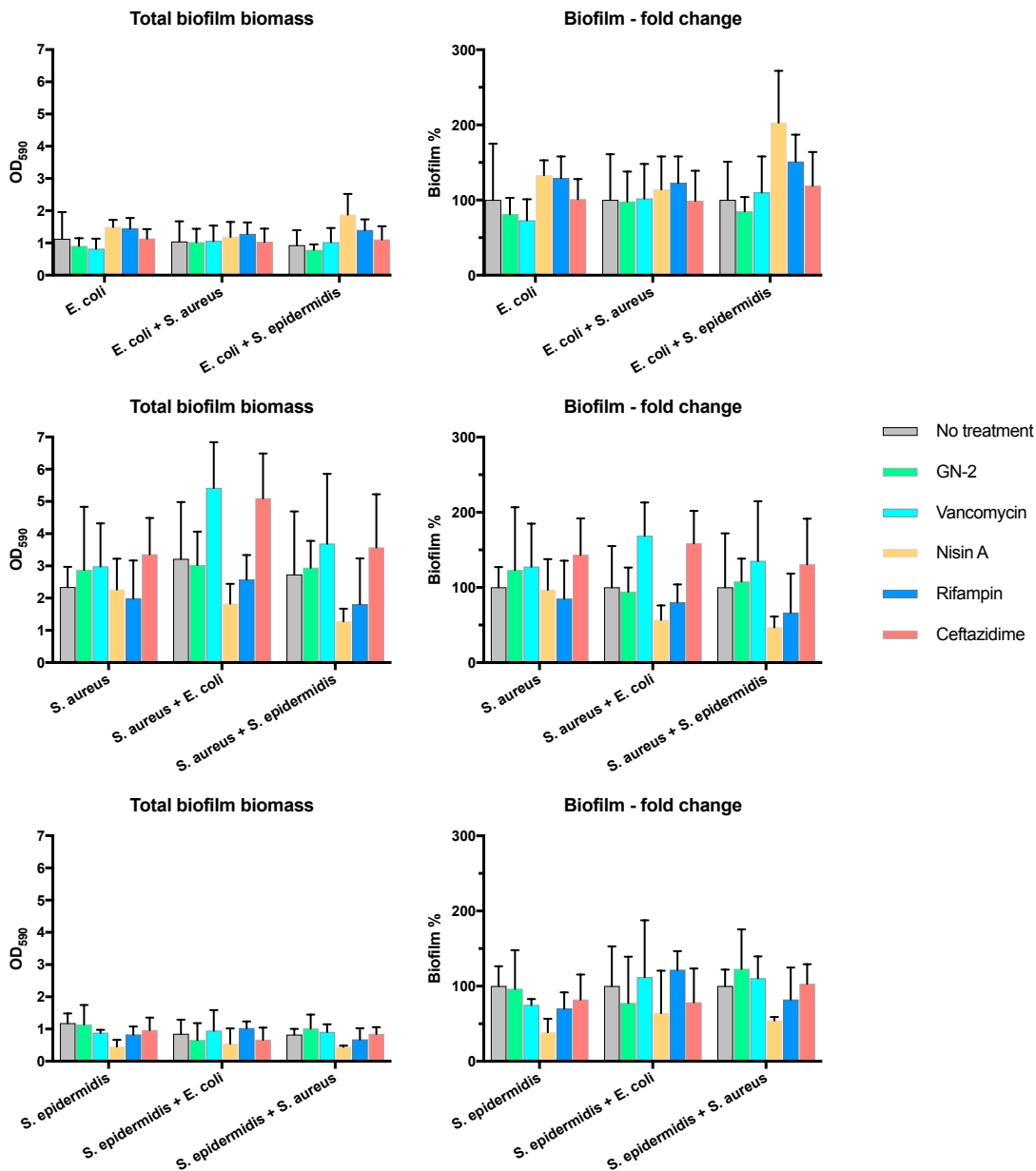


Figure 11 Total biofilm biomass measured by crystal violet staining. Graphs named “Total biofilm biomass” illustrates biomass as colour intensity measured by OD₅₉₀. Graphs named “Biofilm – fold change” illustrates results of measured OD₅₉₀ as fold change compared to the control “No treatment”. Names on the horizontal axes describe combinations of bacteria in the sample where the first mentioned was the first bacteria seeded during biofilm formation. Every sample was made in triplicate (3 consecutive wells) and the assay was repeated three times. Results are giving as means and black bars represent SD values.

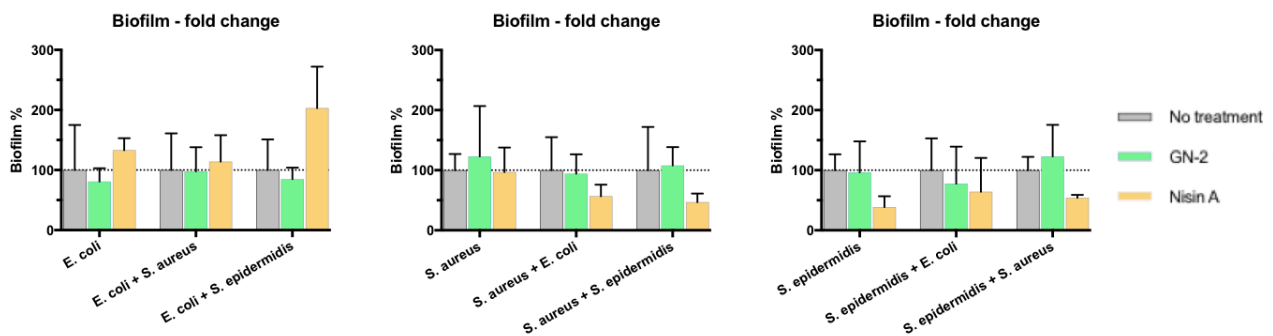


Figure 12 Total biofilm biomass measured by crystal violet staining. Results for GN-2 and nisin A compared to control “No treatment”. Graphs illustrate results of measured OD_{590} as fold change compared to the control “No treatment” which is set at 100%. Names on the horizontal axes describe combinations of bacteria in the sample where the first mentioned was the first bacteria seeded during biofilm formation. Every sample was made in triplicate (3 consecutive wells) and the assay was repeated three times. Results are giving as means and black bars represent SD values.

Biofilm eradication – Bacterial count determined by PMA qPCR

To evaluate the peptide treatment of biofilms the total biomass as well as bacterial counts were assessed. The DNA-binding dye propidium monoazide (PMA) was used to discriminate between viable and non-viable bacteria prior to qPCR amplification. PMA binds to DNA of non-viable bacteria so this DNA cannot be amplified during qPCR. The selective binding of DNA from non-viable bacteria only is possible since PMA cannot penetrate the bacterial membrane of viable bacteria. PMA was tested on viable, non-viable, and mixed planktonic *E. coli*. Results are illustrated in **Figure 13**. The difference between viable “*E. coli*” and mixed “*E. coli* + heat killed” is 1 Ct value which corresponds to a 50% reduction in viable bacterial count concurring with a mix of equal parts viable- and non-viable bacteria. However, the non-viable sample “heat killed” also yielded Ct-values corresponding to approximately 10^4 bacteria when calculated from the standard curve in **Figure 17**. **Figure 14** confirms that no viable bacteria are present in the heat killed sample, so this inaccuracy should be kept in mind when assessing the bacterial counts of biofilm eradication illustrated in **Figure 20** and **Figure 21**.

Also, primer specificity was assessed of the designed primers used in this thesis. Since *S. aureus* and *S. epidermidis* have high genomic homology, specificity for these two primers were assessed and are illustrated in **Figure 15** and **Figure 16**. Specificity was not 100% for the *S. aureus* 149 primer as illustrated by Ct-values from the *S. epidermidis* bacteria sample (**Figure 15**). This inaccuracy could also affect results of bacterial counts of biofilm eradication illustrated in **Figure 20** and **Figure 21**, and this is probably the reason for *S. aureus* bacteria observed in samples where no *S. aureus* should be found - “*S. epidermidis*” and “*S. epidermidis* + *E. coli*” in **Figure 20** and **Figure 21**.

Results of bacterial counts from biofilm eradication assays are illustrated in **Figure 20** and **Figure 21**. The three replicates from the biofilm eradication assay were pooled for qPCR measurement to circumvent the high SD values seen in the crystal violet staining. **Figure 20** shows viable bacterial counts of each biofilm type, single- or multi-species. Results from GN-2 and nisin A have been selected and illustrated as fold change compared to “No treatment” in **Figure 21**. Results of bacterial count correlate with total biomass for GN-2 as it shows a minor decrease in biofilm bacteria in most biofilms where staphylococci are seeded first (**Figure 21**). Nisin A shows greater eradicating effects on almost every type of biofilm with more than a 10 fold reduction of viable bacteria in some cases (**Figure 21**).

PMA test

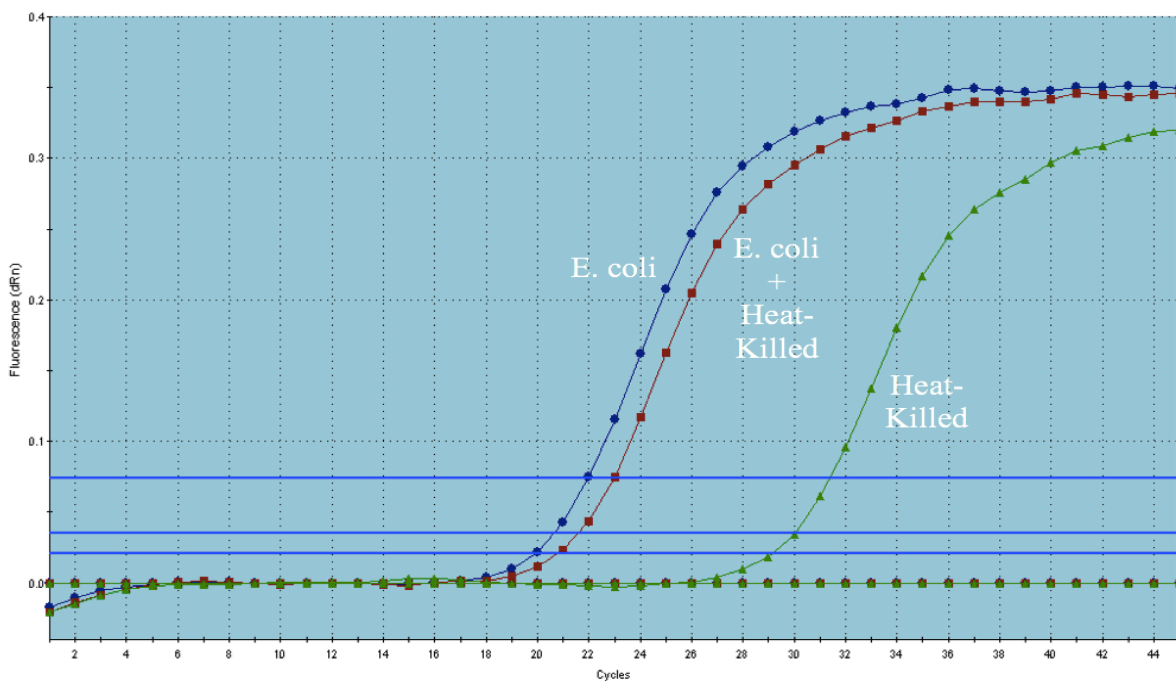


Figure 13 PMA test - Amplification curves from qPCR of planktonic viable- and non-viable *E. coli* samples. Threshold is illustrated by the upper blue line (please disregard the other two). DNA for qPCR amplification was extracted from samples containing *E. coli* inoculums of approximately 10^7 bacteria. Heat-killed bacteria were heated at 99°C for ten minutes. *E. coli* primer listed in Table 5 and qPCR program in Table 6 was applied.

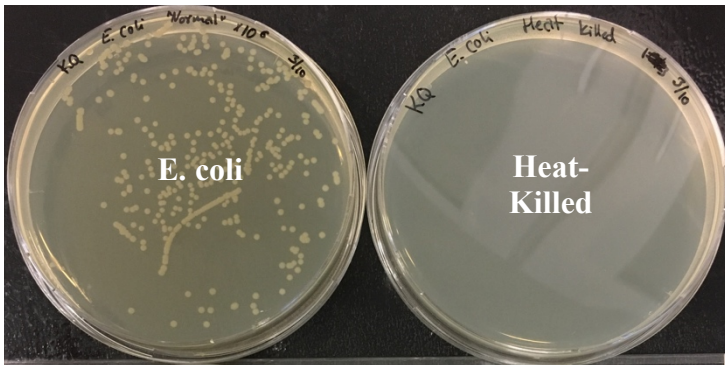


Figure 14 PMA test - LB plates illustrating viable- "E. coli" and non-viable "Heat-Killed" bacterial samples. 100 μ l inoculum diluted 10^{-7} were plated for E. coli. 100 μ l undiluted inoculum were plated for Heat-Killed E. coli. Heat-killed bacteria were heated at 99°C for ten minutes.

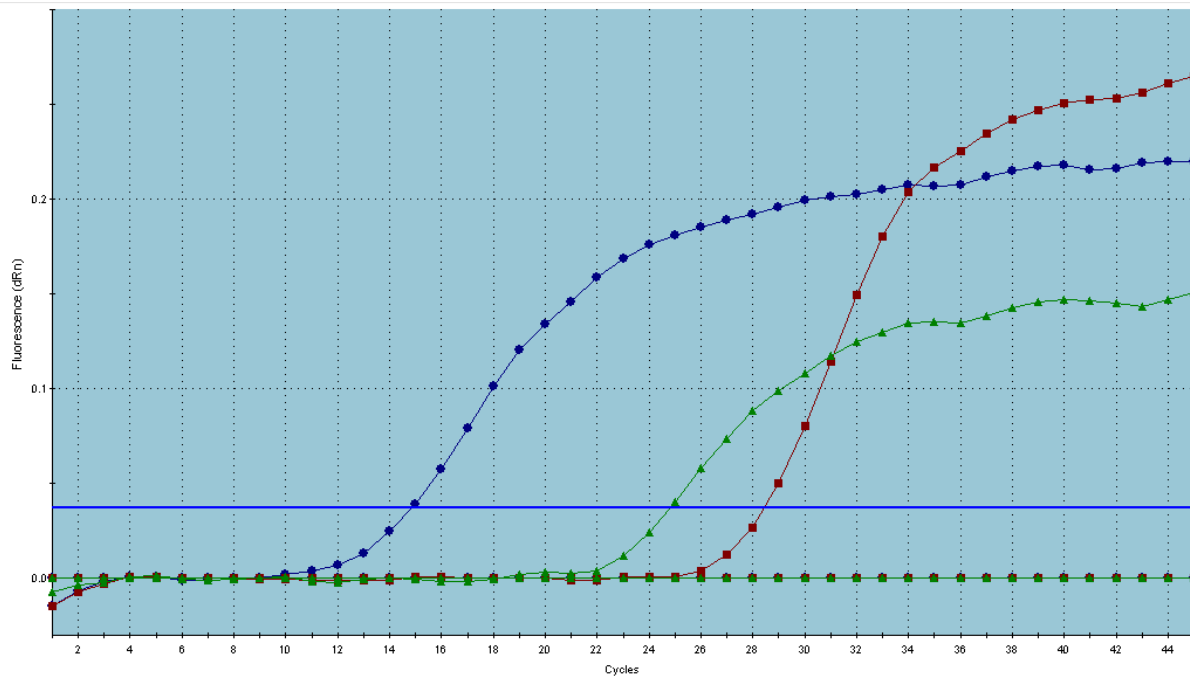


Figure 15 Primer S. aureus 149. Amplification curves from qPCR. S. aureus 149 primer listed in Table 5 and qPCR program in Table 6 was applied. Blue: S. aureus. Green: S. epidermidis. Red: S. lugdunensis (from preliminary bacterial tests). Blue horizontal line marks threshold.

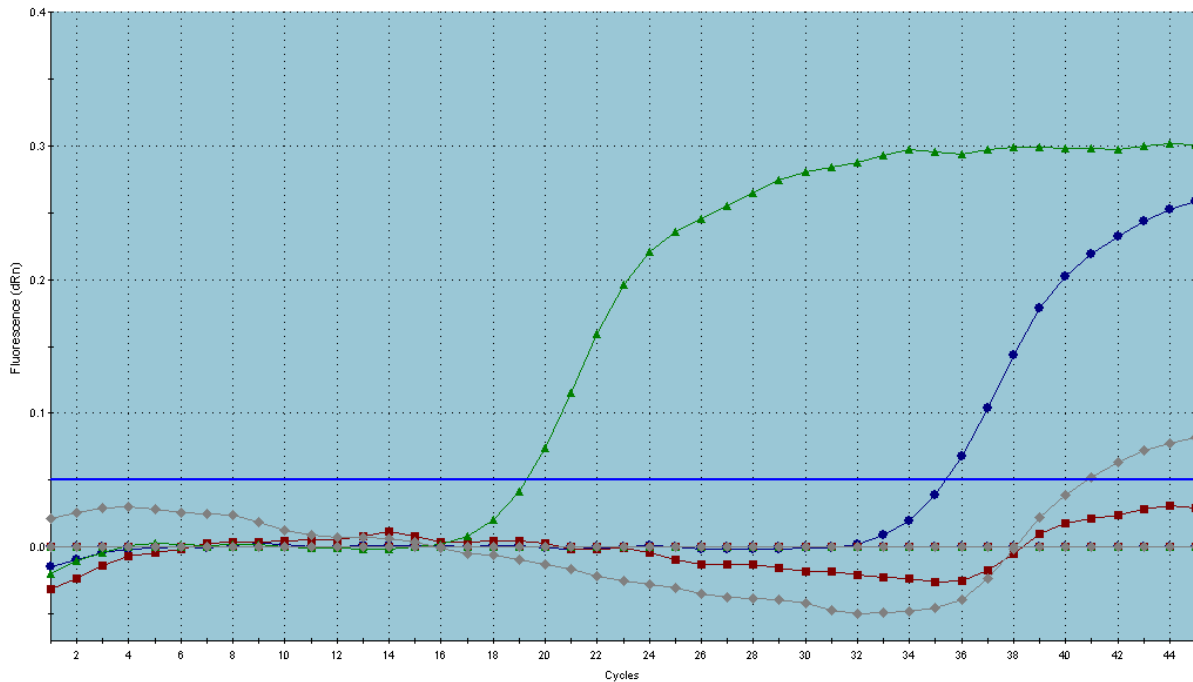


Figure 16 Primer *S. epidermidis* 193. Amplification curves from qPCR. *S. epidermidis* 193 primer listed in Table 5 and qPCR program in Table 6 was applied. Blue: *S. aureus*. Green: *S. epidermidis*. Red: *S. lugdunensis* (from preliminary bacterial tests). Blue horizontal line marks threshold

Standard curves

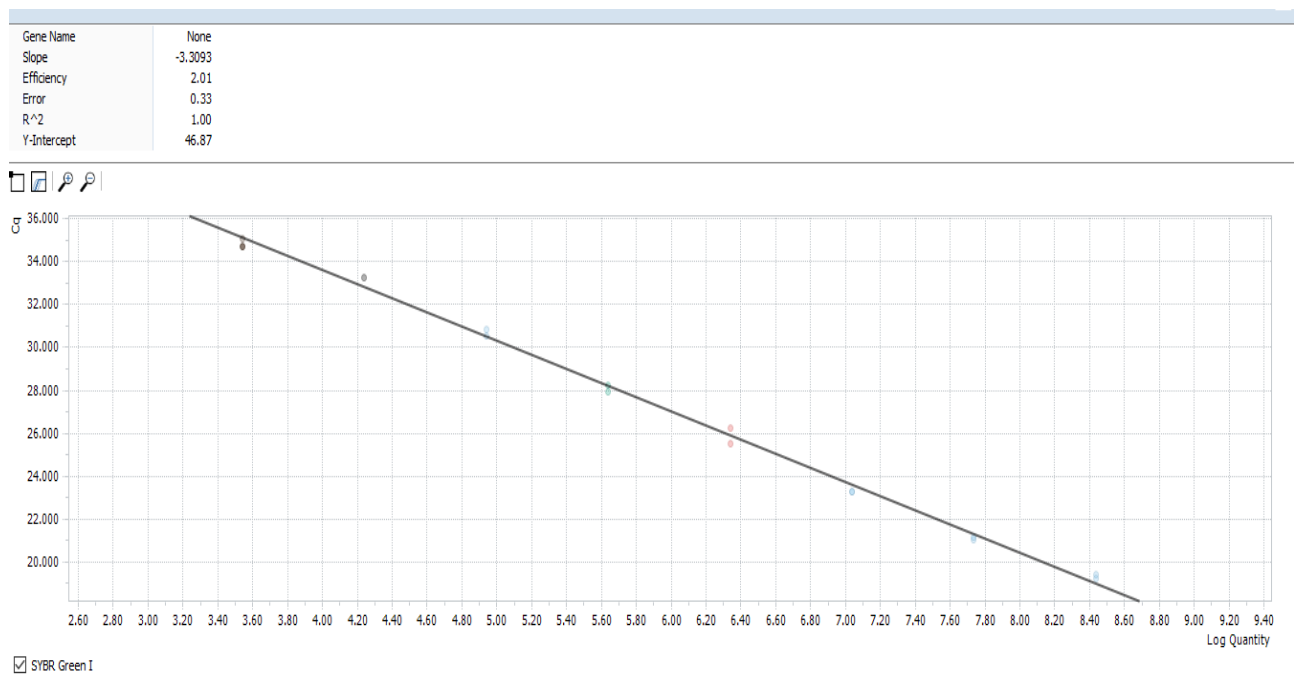


Figure 17 Standard curve for *E. coli*. Standard curves were made from serial dilutions of samples containing planktonic bacteria of known values. Only Ct-values inside the linear spectrum of the standard curves were included in the results of bacterial count illustrated in Figure 20 and Figure 21. *E. coli* primer listed in Table 5 and qPCR program in Table 6 was applied

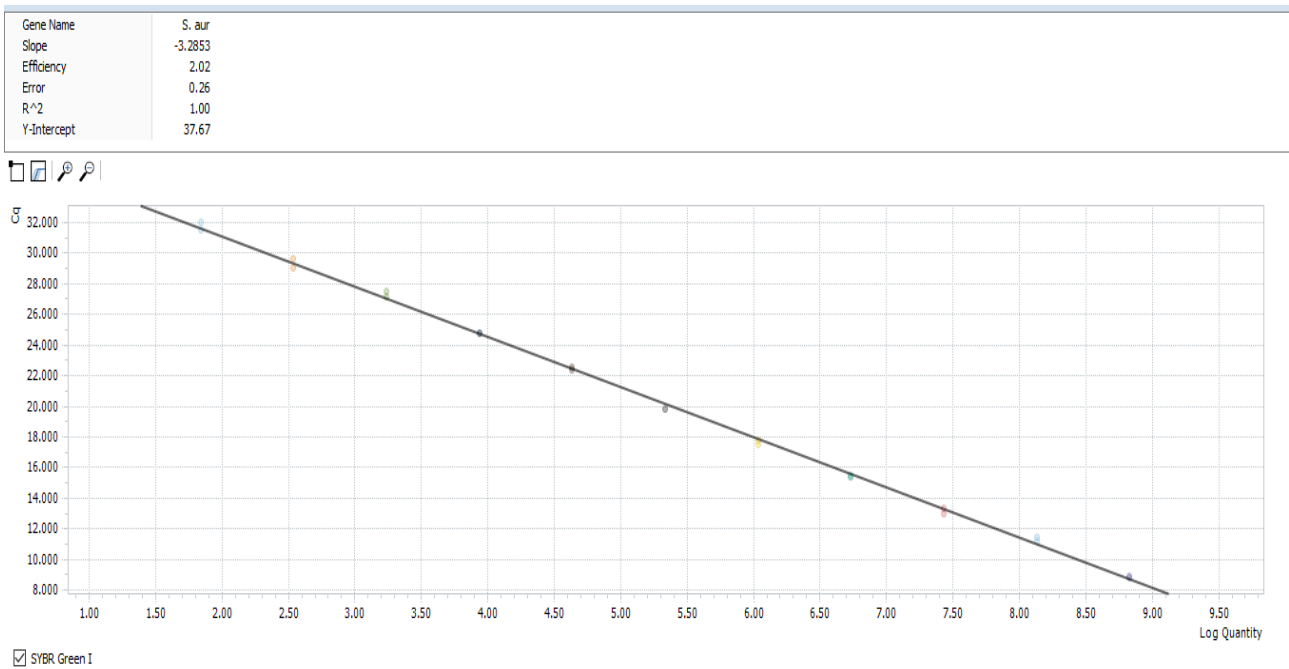


Figure 18 Standard curve for *S. aureus* 149. Standard curves were made from serial dilutions of samples containing planktonic bacteria of known values. Only Ct-values inside the linear spectrum of the standard curves were included in the results of bacterial count illustrated in Figure 20 and Figure 21. *S. aureus* 149 primer listed in Table 5 and qPCR program in Table 6 was applied.

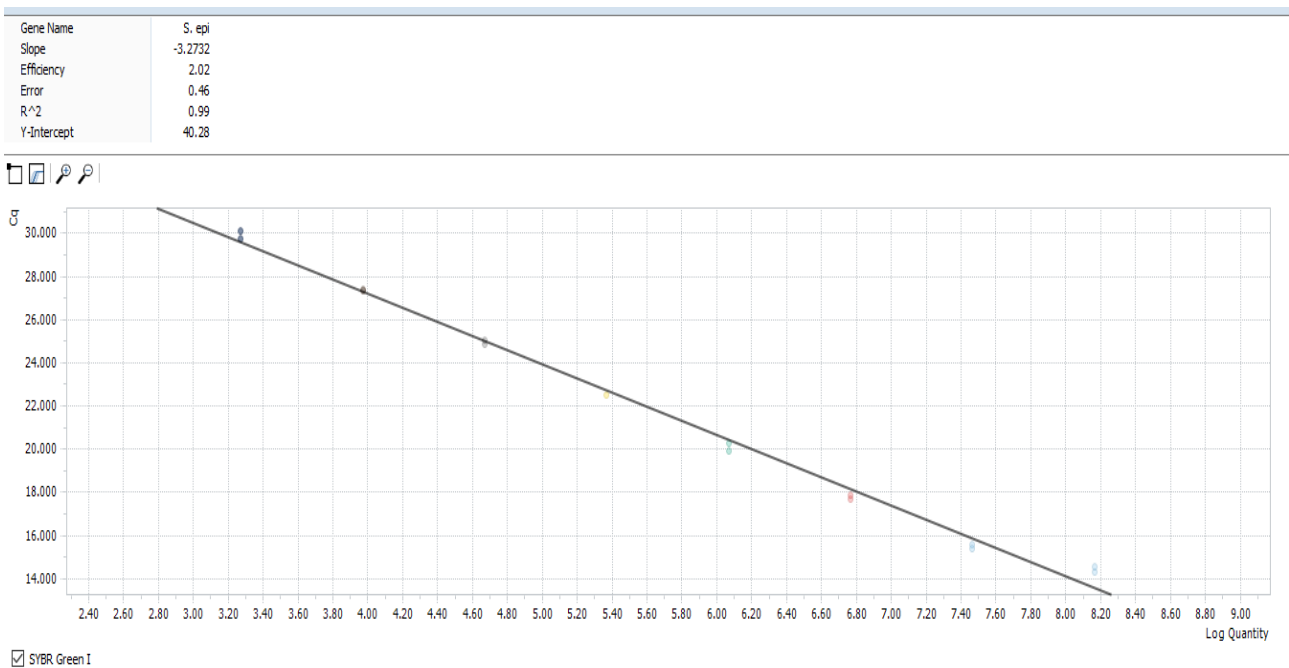


Figure 19 Standard curve for *S. epidermidis* 193. Standard curves were made from serial dilutions of samples containing planktonic bacteria of known values. Only Ct-values inside the linear spectrum of the standard curves were included in the results of bacterial count illustrated in Figure 20 and Figure 21. *S. epidermidis* 193 primer listed in Table 5 and qPCR program in Table 6 was applied.

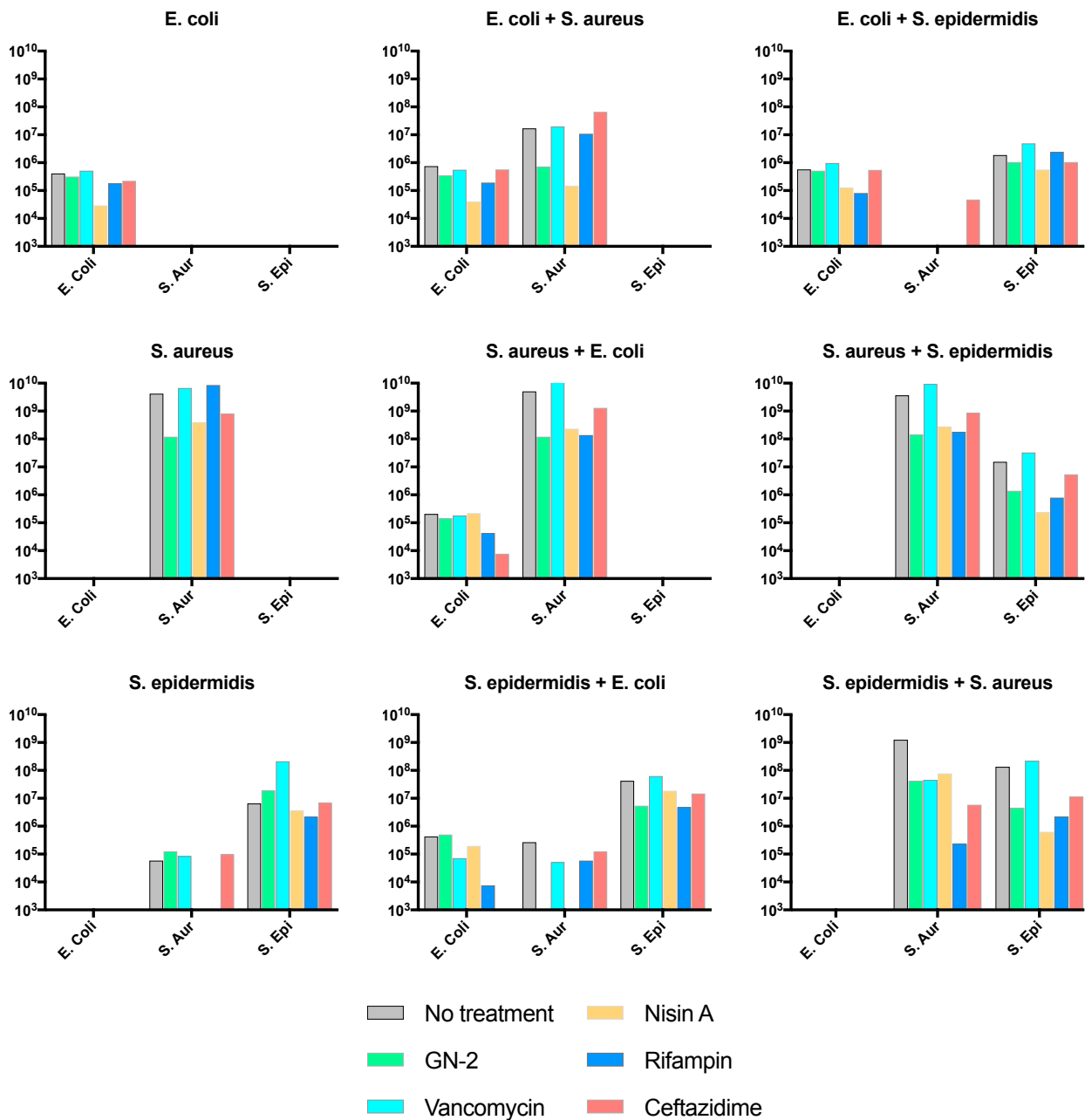


Figure 20 Viable bacterial counts of each biofilm type, single- or multi-species, determined by qPCR. Primers listed in Table 5 and qPCR program in Table 6 was applied The three replicates from the biofilm eradication assay were pooled for qPCR measurement. Y-axis: bacterial number. Name of each graph describe combinations of bacteria in the sample where the first mentioned was the first bacteria seeded during biofilm formation. Horizontal axes name the bacteria determined by corresponding bacterial primer. The assay was conducted only 1 time and therefor no SD bars or calculations of significance are applied. Results are calculated using standard curves made from dilutions of planktonic viable bacteria of known values seen in Figure 17, Figure 18, and Figure 19.

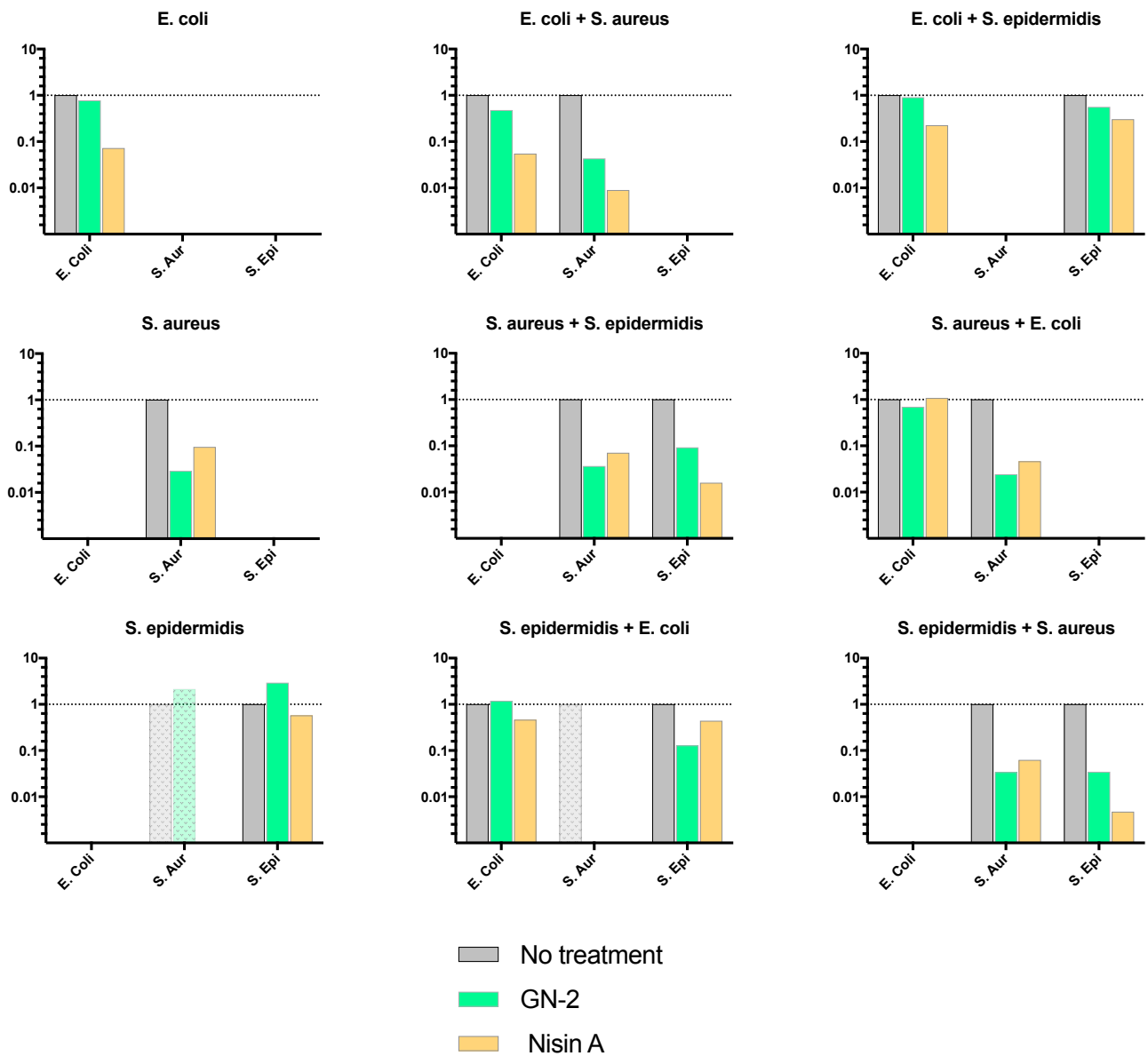


Figure 21 Bacterial counts fold change Nisin + GN-2 Viable bacterial counts for GN-2 and nisin A of each biofilm type, single- or multi-species, determined by qPCR. Primers listed in Table 5 and qPCR program in Table 6 was applied The three replicates from the biofilm eradication assay were pooled for qPCR measurement. Y-axis: fold change in bacterial number. Name of each graph describe combinations of bacteria in the sample where the first mentioned was the first bacteria seeded during biofilm formation. Horizontal axes name the bacteria determined by corresponding bacterial primer. The assay was conducted only 1 time and therefor no SD bars or calculations of significance are applied. Results are calculated using standard curves made from dilutions of planktonic viable bacteria of known values seen in Figure 17, Figure 18, and Figure 19. Less transparent bars illustrate analytical insecurities mentioned earlier in the section “Biofilm eradication – Bacterial count determined by PMA qPCR”.

Wound healing

To further characterise the AMPs of this study, their immunomodulatory effects were studied as well. For this, an *ex-vivo* wound healing model utilizing skin from pig's ears was applied. This model was used to assess wound healing properties of GN-2, nisin A, NT, and SP after one and three days of peptide treatment. Skin was washed and sterilized with 70% ethanol before infliction of wounds with a 2 mm diameter biopsy punch. After wounding (time 0) skin pieces were placed in DMEM containing different AMPs at a concentration of 25 µg/ml. Peptide-containing DMEM was poured over the skin pieces placed on gauze in a 12-well plate so the wound area was soaked and the well was filled with media to a point where only the epithelial layer was above the air-liquid interphase. Peptide-containing DMEM was changed every 24 h. Samples were taken at three time points (time 0, day 1 and day 3) and fixed in 4% paraformaldehyde. Samples were embedded in paraffin and sectioned before staining.

Wound healing properties of the four AMPs were studied by light microscopic evaluation and measurements of stained cross-sections from wounds. Histology was evaluated by H&E staining and proliferating cells were identified by immunohistochemical staining with ki67 antibody. Measurements, explained in **Figure 28**, were made by Associate Professor Steen Seier Poulsen at Copenhagen University.

Every wound was completely covered by a new epithelial layer at day three illustrated in **Figure 22** and **Figure 24** demonstrating viability of porcine skin cells three days after excision. From the results combined in **Figure 29**, it appears that the two known antimicrobial peptides GN-2 and nisin A have a positive effect on early stages of wound healing, illustrated by more epithelial ingrowth on day 1 compared to a no treatment control. This suggests an effect on epithelial migration by GN-2 and especially nisin A. On day three NT and SP, on the other hand, seemed to have an effect illustrated by thicker epithelial layer and more proliferating cells.

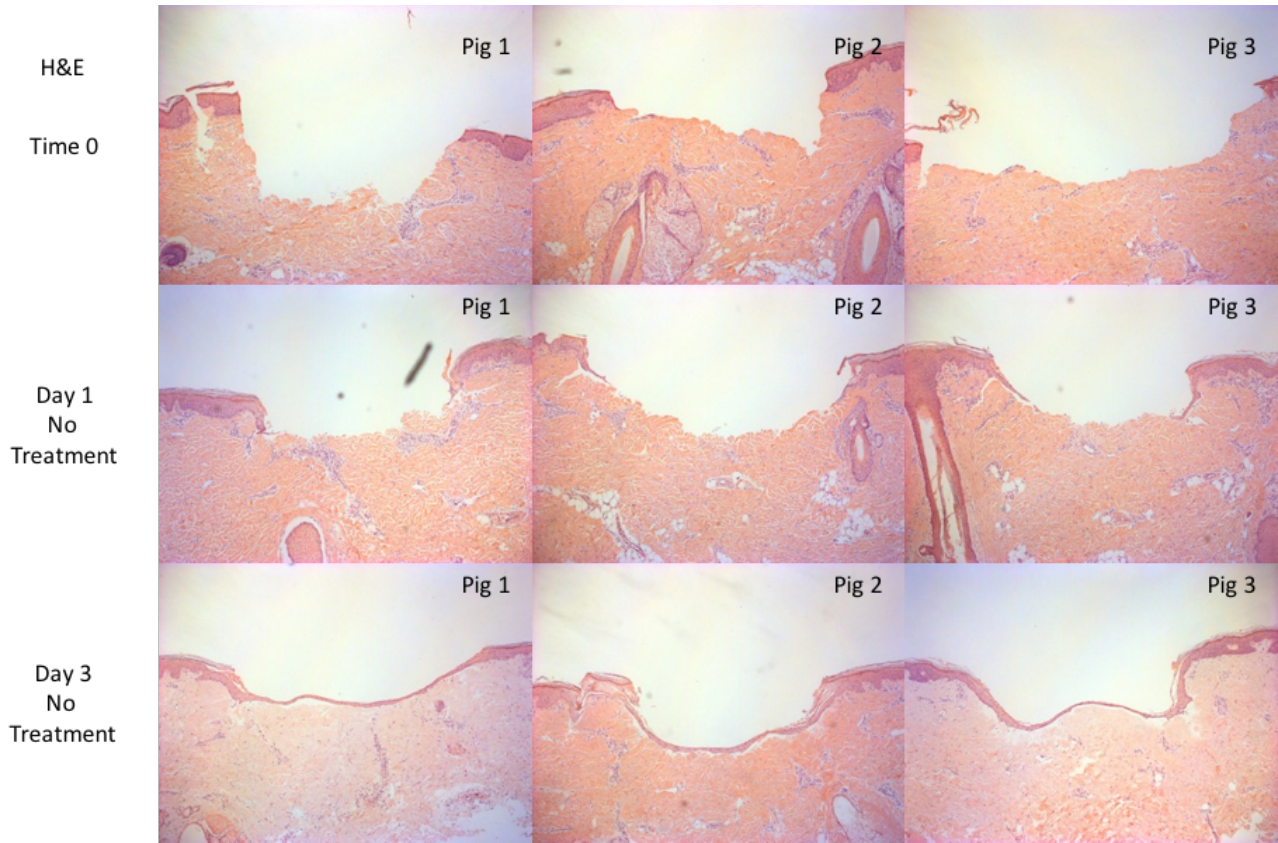


Figure 22 Wounds from day 0 to day 3 without peptide treatment. H&E staining. 5x magnification. Each treatment is tested in triplicates on skin from three different pig's ears (pig 1, 2, and 3). Notice the complete coverage of the wound site by newly formed epithelia on day three.

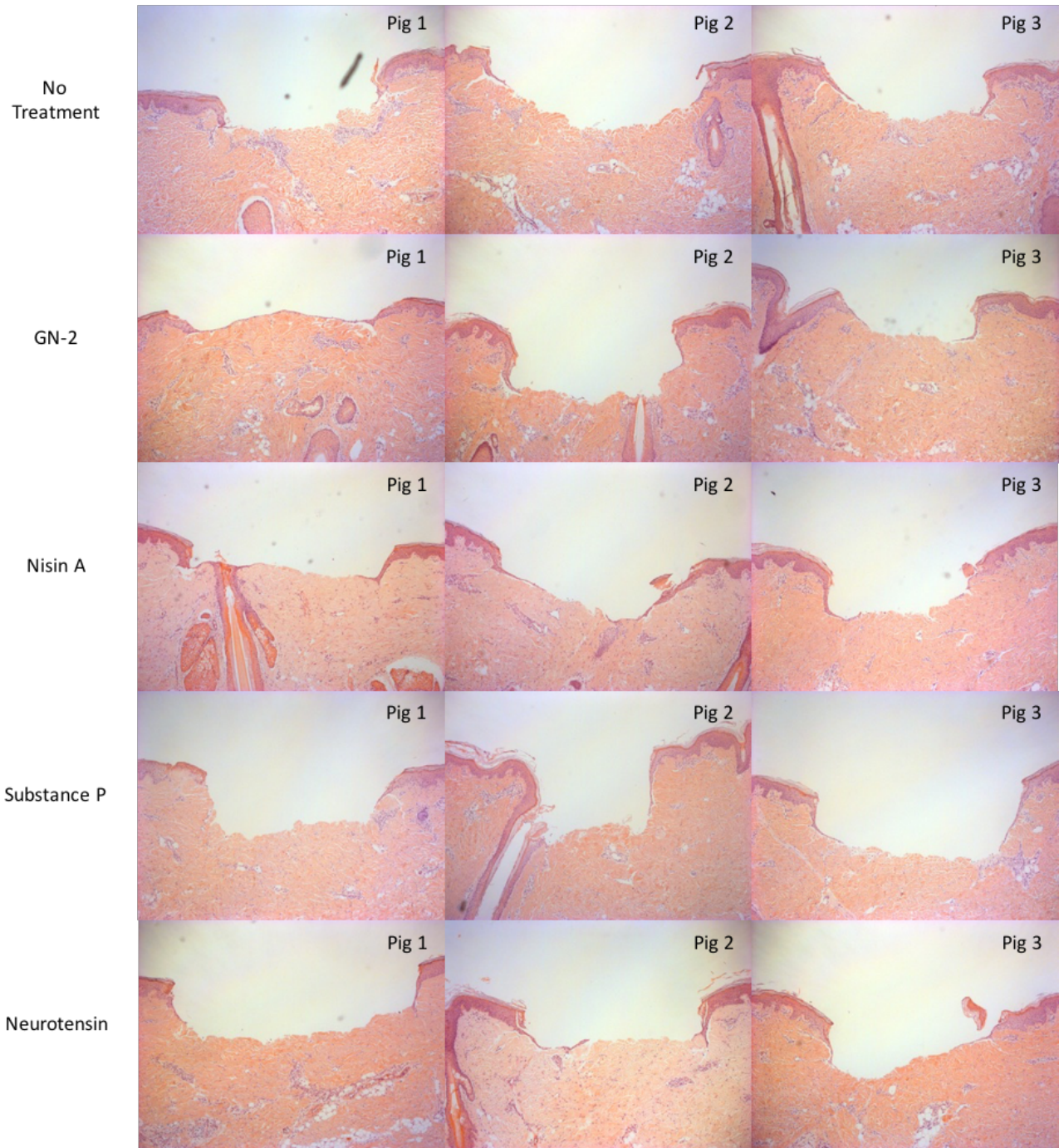


Figure 23 Wounds with different peptide treatment on day 1. H&E staining. 5x magnification. Each treatment is tested in triplicates on skin from three different pig's ears (pig 1, 2, and 3). Hair follicles are observed in some wounds and consequently, the epithelial cells lining the follicles can contribute to the newly formed layer of epithelia. This has been considered when measuring epithelial ingrowth illustrated in Table 7 and Figure 29.

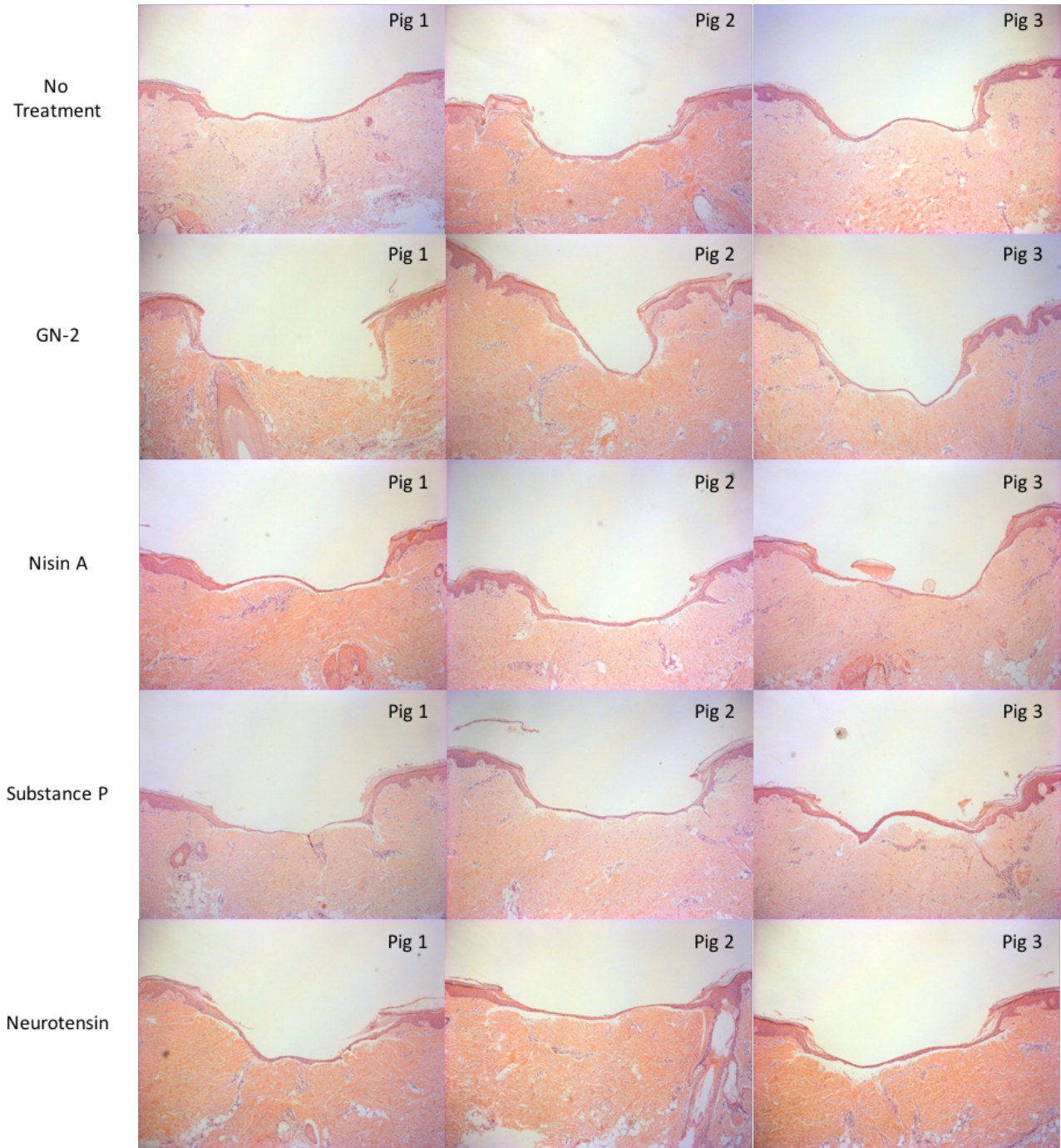


Figure 24 Wounds with different peptide treatment on day 3. H&E staining. 5x magnification. Each treatment is tested in triplicates on skin from three different pig's ears (pig 1, 2, and 3). Hair follicles are observed in some wounds and consequently, the epithelial cells lining the follicles can contribute to the newly formed layer of epithelia. Measurements of wound with and newly formed epithelial depth are illustrated in Table 7 and Figure 29.

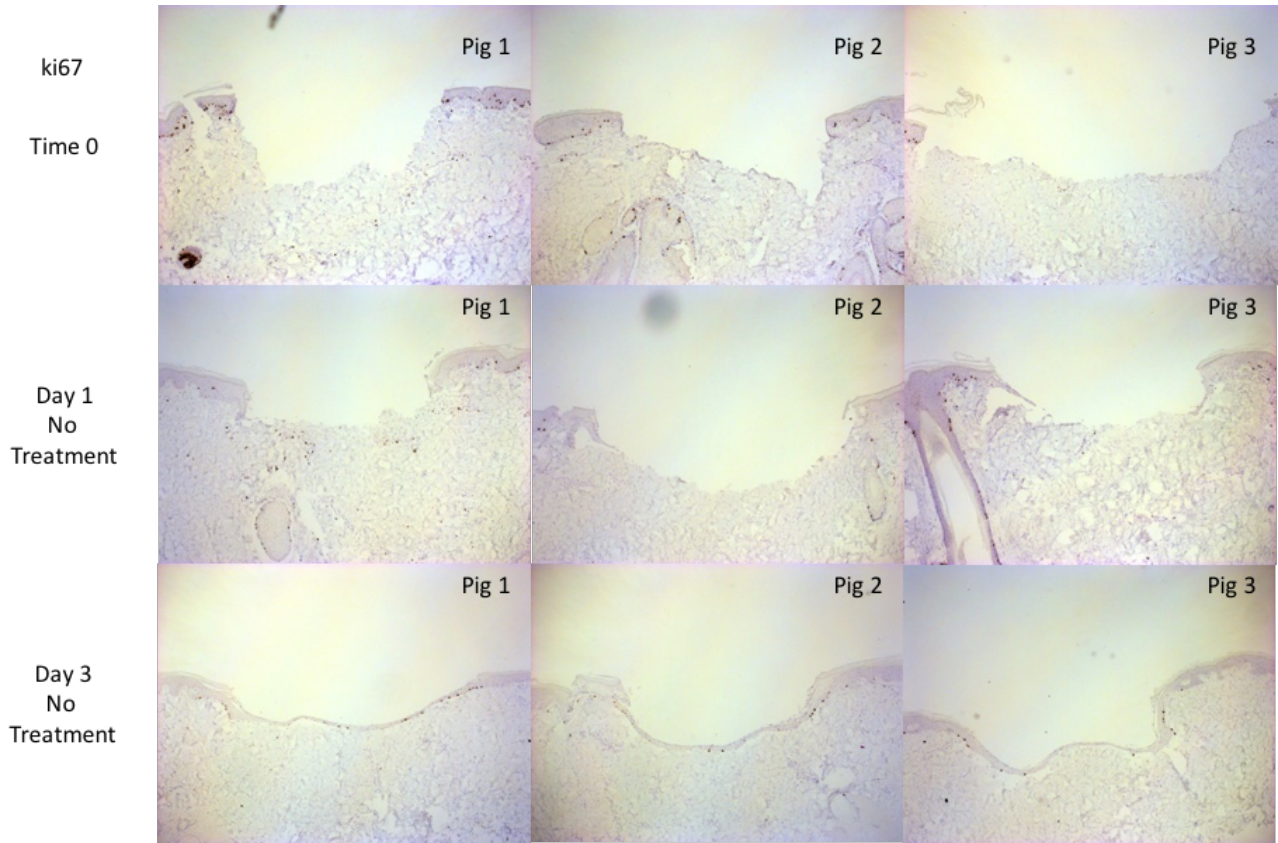


Figure 25 Wounds without treatment on day 0 to day 3. Ki67 staining. 5x magnification. Each treatment is tested in triplicates on skin from three different pig's ears (pig 1, 2, and 3). Proliferating cells are stained by the ki67 antibody, illustrated by the dark brown spots in these pictures.

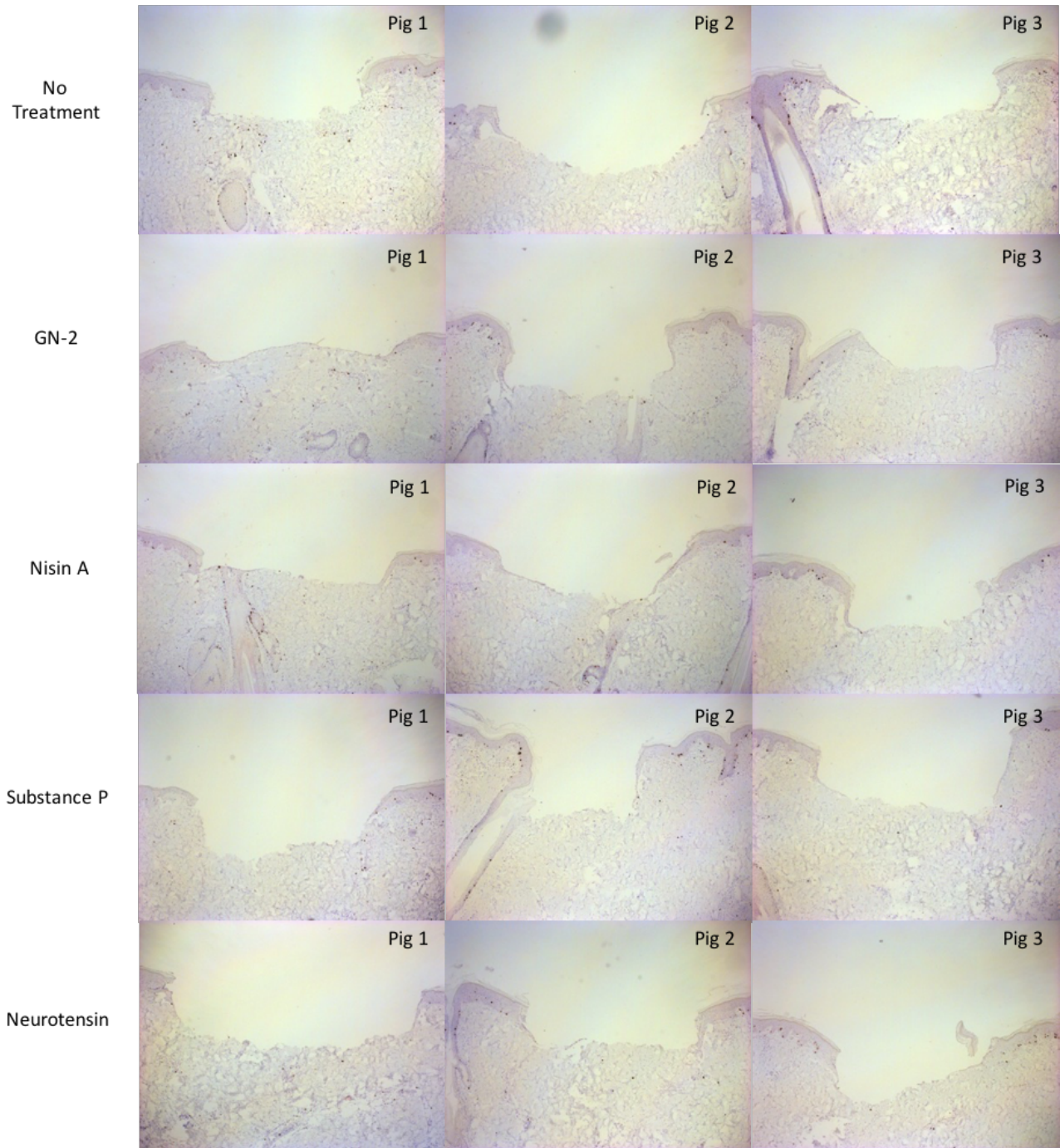


Figure 26 Wounds with different peptide treatments on day 1. Ki67 staining. 5x magnification. Each treatment is tested in triplicates on skin from three different pig's ears (pig 1, 2, and 3). Measurements of proliferating cells inside the wound area, illustrated by the dark brown spots of ki67 staining in these pictures, are seen in Table 7.

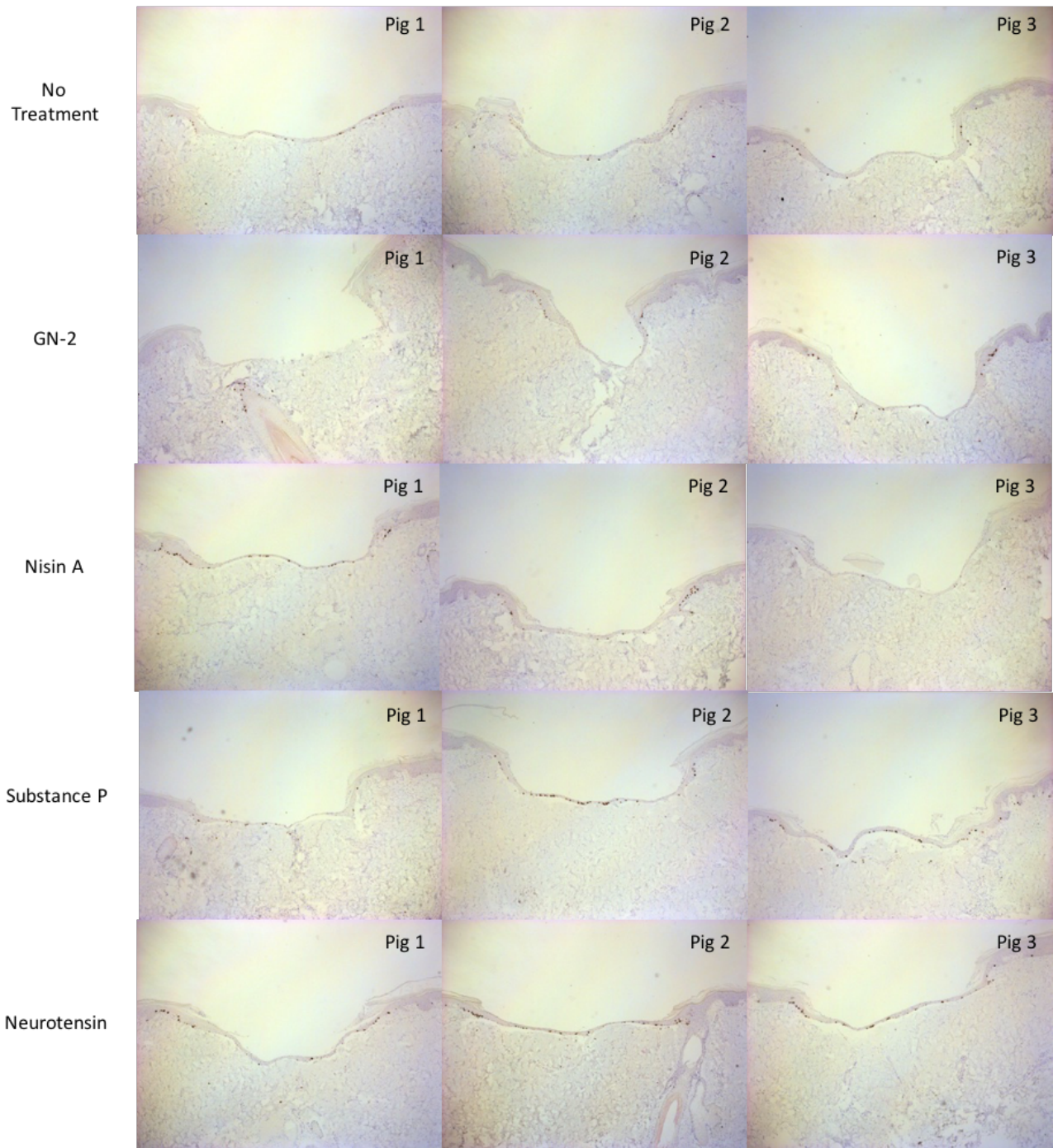


Figure 27 Wounds with different peptide treatments on day 3. Ki67 staining. 5x magnification. Each treatment is tested in triplicates on skin from three different pig's ears (pig 1, 2, and 3). Measurements of proliferating cells inside the wound area, illustrated by the dark brown spots of ki67 staining in these pictures, are seen in Table 7 and in Figure 29.

Table 7 Wound width, epithelial ingrowth, epithelial depth and ki67-positive cells from wounds represented in Figure 22 Figure 29.

Pig no.	Wound width (mm)				Epithelial ingrowth (mm)				Epithelial depths (mid wound) (µm)				ki67 positive cells in wound			
	1	2	3	Mean	1	2	3	Mean	1	2	3	Mean	1	2	3	Mean
Day 0																
Control	2,4	2,3	3,7	2,8												
Day 1																
Control	1,9	2,3	1,8	2,0	0,32	0,51	0,70	0,51					0	0	0	0
GN2	1,3	1,9	1,5	1,6	1,28	0,90	0,83	1,00					0	0	0	0
Nisin A	2,2	2,1	1,7	2,0	1,15	1,22	0,83	1,07					1	1	1	1
SP	2,1	1,3	2,2	1,8	0,26	0,64	1,22	0,70					1	2	0	1
NT	2,7	2,1	1,9	2,2	0,64	1,15	0,70	0,83					0	0	0	0
Day 3																
Control	2,3	2,1	2,2	2,2	2,31	2,18	2,43	2,31	38	38	19	32	12	12	7	10
GN2	2,1	1,0*	1,8	1,6	2,05	1,92	2,18	2,05	13	19	13	15	0	4	9	4
Nisin A	2,2	1,9	2,2	2,1	2,31	2,31	2,56	2,39	19	32	26	26	17	9	3	10
SP	1,8	2,1	1,9	1,9	1,92	2,43	2,31	2,22	13	19	51	28	9	28	23	20
NT	1,9	2,1	2,2	2,1	2,18	2,24	2,31	2,24	38	32	51	41	12	25	21	19

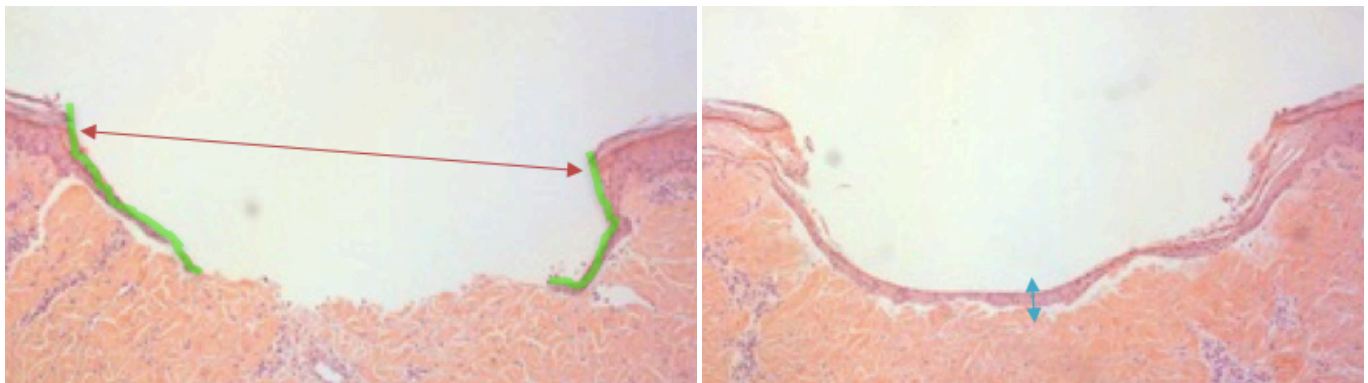


Figure 28 Illustrations of wound healing measurements applied in Table 7. Red arrow represents wound width. Green marking represents epithelial ingrowth. Blue arrow represents depth of newly formed epithelium.

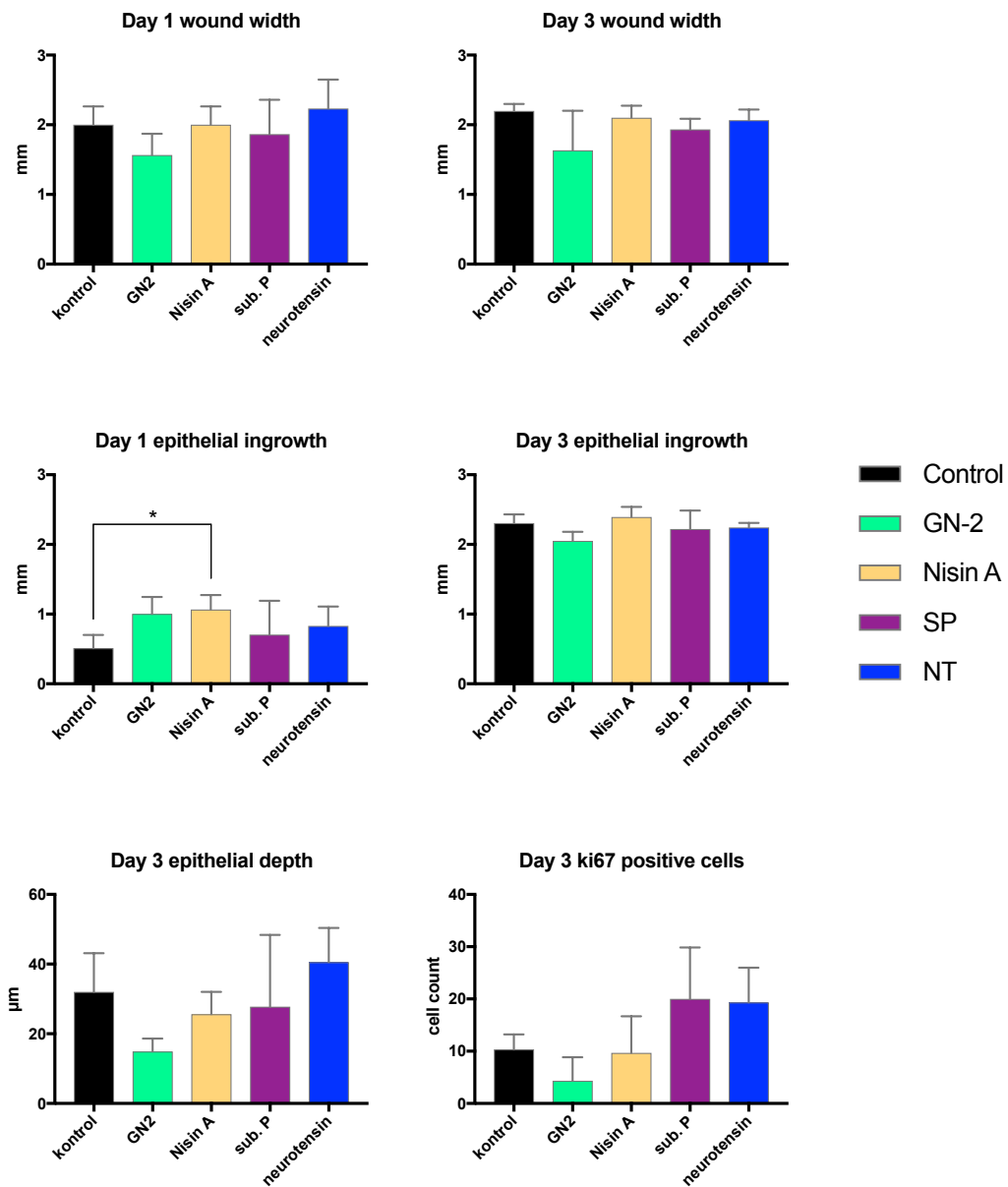


Figure 29 Selected results from Table 7 illustrated as bar graphs. Wound width (mm), epithelial ingrowth (mm), epithelial depth (μm) and ki67-positive cells of wounds treated with different peptides represented in Figure 22. Each treatment is tested in triplicates on skin from three different pig's ears. Results are given in mean + SD. *P = 0,0267.

Discussion

DFU is a critical long term complication of diabetes, that due to the large number of diabetes incidents is also a vast economic burden in healthcare world-wide. DFU is categorised as a non-healing wound often infected by multiple species of biofilm forming bacteria⁵¹. As a new potential candidate for the treatment of DFU and other chronic wounds AMPs have been contemplated due to their potential antimicrobial and immunomodulating abilities³⁴. In this thesis, different AMPs were evaluated on their effect on biofilm eradication and wound healing. Biofilm eradication effect was studied by a microtiter dish biofilm formation assay followed by treatment with AMPs and then two different ways of quantifying biofilm eradication; 1) by staining of total biofilm biomass by crystal violet 2) by qPCR with species-specific primers on PMA treated biofilms to quantify total number of viable bacteria after antimicrobial treatment. The immunomodulatory effects of AMPs and their effect on wound healing was studied using an *ex-vivo* porcine skin model, that was developed and modified through the span of this work. The observed antimicrobial and wound healing properties of the AMPs and their potentials as therapeutic agents for the treatment of DFU will be discussed in the following.

Biofilm eradicating effects of AMPs

Biofilm production is a virulence factor and survival mechanism for several bacteria. The organization into communities of tightly packed bacteria embedded in a sticky extracellular matrix offers an effective protection against antimicrobial substances. This trait results in more and more bacterial strains being resistant towards the commonly used antibiotics in our health care systems. By the results of the performed biofilm eradication assays we clearly observe how even extremely high doses of three common antibiotics are almost completely ineffective against the mature biofilms. Vancomycin, rifampin and ceftazidime are used in concentrations of more than 100 times their MIC values for planktonic bacteria. The *S. epidermidis* strain ET-024 is reported methicillin resistant which explains the high tolerance towards beta-lactams and cephalosporins like ceftazidime, but rifampin and vancomycin also have very little effect on the biofilm formed by this bacterium. Vancomycin acts by inhibition of the cell wall synthesis. The cell wall of bacteria is constantly being renewed during their lifecycle and the synthesis of new cell wall components and the cross-linking of these are necessary to maintain the barrier function of the membrane and to sustain viability. By this theory vancomycin should be able to kill both Gram-positive staphylococci here but for vancomycin to exert its effect it must be able to reach and interact with the bacterium and this is where the complex structure of biofilm could be an obstacle. Bacteria in the middle of a mature

biofilm are protected by the surrounding bacteria and the components of the extracellular matrix. This could explain the inability of vancomycin to eradicate preformed biofilm. Okuda, on the other hand, showed that vancomycin actually is able to penetrate biofilms made by *S. aureus*⁵². This was illustrated in biofilms treated with fluorescently labelled vancomycin. After just 60 min. the biofilm was dissolved and observed by fluorescent microscopy showing fluorescence at the surface of virtually every bacterium. This proves that vancomycin can penetrate *S. aureus* biofilm. So why is it, that vancomycin is not able to exert its bactericidal effect on bacteria in biofilms? – The slow growth-rate of bacteria in the inner part of biofilms are believed to be the answer since the process of cross-linking of newly synthesized peptidoglycans must be active for vancomycin to exert its effect^{53,54}. The architectural structure of biofilms is illustrated in **Figure 2**. This slow growth-rate is also the reason why rifampicin has low effect on biofilm since it inhibits the transcription of mRNA.

Two of the selected AMPs were tested for biofilm eradication effects. Nisin A and GN-2. These AMPs were selected based on their shown antimicrobial activities and low cytotoxicity, making them suitable therapeutic candidates for the treatment of infected wounds. Nisin A is an AMP naturally produced by the bacteria *Lactococcus lactis*. It has been shown to exert antimicrobial effects on a number of Gram-positive bacteria including methicillin resistant *S. aureus* strains³³. GN-2 is a synthetically produced AMP which antimicrobial properties have also been shown against both *S. aureus* and *E. coli*³⁴.

GN-2

GN-2 is relatively new in the field of AMPs and not yet thoroughly characterized. It was synthesized and described by Fjell *et al.* in 2011. A library of GN-peptides was evaluated and GN-2 was found the best candidate with broad spectrum antimicrobial activity against both Gram-negative *E. coli* and Gram-positive *S. aureus*. GN-2 showed superior selectivity towards bacterial versus mammalian cells³⁷ and a potent and rapid antibacterial effect on *E. coli* (MIC= 16 µg/ml) and *S. aureus* (MIC= 4-8 µg/ml)³⁴. Saporito *et al* shows that GN-2 also has a small biofilm eradicating effect on *E. coli* biofilms. A 10% reduction of biofilm biomass was reported at 64 µg/ml against an *E. coli* biofilm⁵⁵. In the corresponding assay of this study a very small reduction in *E. coli* biofilm biomass was also observed at the same peptide concentration – confer the single species “*E. coli*” sample in **Figure 12**. although as earlier mentioned no values were significant according to unpaired t-test. Interestingly, PMA qPCR results show a decrease in bacterial count of *S. aureus* and *S. epidermidis* after GN-2

treatment in every sample except for the single-species “*S. epidermidis*” sample (**Figure 21**). This result might suggest that GN-2 is able to kill some bacteria in a biofilm but maybe these non-viable bacteria are still lodged in the biofilm matrix, and therefore a reduction in complete biomass is not observed by CV staining or only observed in a lesser degree. Regarding the mode of action of GN-2 no exact mechanism has yet been elucidated, but several findings suggests membrane permeabilization as the main action of this peptide^{34,55,56}. Both membrane permeabilization and interactions with intracellular targets requires the peptide to be in close proximity to the bacterial cell to exert its antibacterial effect. The tight structure of biofilms and the components of the extracellular matrix evidently makes it difficult for substances to reach the inner bacteria of a biofilm, and thereby illustrating the big difference between planktonic and biofilm killing activity. Saporito et al. showed that GN-2 is only able to penetrate the outer membrane of *E. coli*, and maybe therefore, the effect on the staphylococci biofilms are slightly more evident, since these bacteria only have one membrane, although thicker in structure⁵⁷.

In the study by Saporito, the GN-2 peptide is compared with a corresponding peptoid version. This modified more hydrophobic peptoid showed greater effect on biofilm eradication but also less effect on planktonic *E. coli*⁵⁷. This suggests that the two probably have different mode of actions, and it might be, that the modified structure and hydrophobicity is the reason why the peptoid can penetrate the inner membrane and eradicate 5 times more biofilm than the GN-2 peptide. As the suggested mode of action for GN-2 is direct membrane penetration it would not be expected, but it could also be the same problem as described earlier for vancomycin, that the dormant bacteria are not affected as much as the viable bacteria due to low metabolism. If this is the case, then an alternative mode of action for GN-2 could be speculated together with the membrane penetrating effect.

Nisin A

Nisin has been utilized as a preservative in the food industry for several years, due to its antimicrobial properties. It is completely safe to use and it was approved by the FDA in 1988⁵⁸. Several reports have described the antimicrobial properties of nisin towards Gram-positive bacteria and found MIC values ranging from 0,01 to 83,6 µg/ml³³. Nisin’s effect on biofilm eradication has also been reported. Okuda et al. shows that nisin A has a significant eradicating effect on biofilms of methicillin-resistant *S. aureus* (MRSA) at peptide concentration of 64 µg/ml (8xMIC)⁵². Field et al. also shows an eradication effect on *S. aureus* biofilms at 50 µg/ml (6xMIC)⁵⁹. Looking at the results from crystal violet staining (total biomass) in this study, it seems that nisin A has an effect on all but one of samples

where staphylococci is the first bacteria to be seeded in the wells (**Figure 12**) (second bacteria were seeded after 4 h). In the wells where *E. coli* are seeded first nisin A has no effect on biomass. Almost, a biofilm-enhancing effect is seen in some cases (**Figure 12** “*E. coli* + *S. epidermidis*”). This correlates with earlier findings demonstrating that nisin A has superior effect on Gram-positive bacteria⁶⁰. When conferring the results of viable bacterial count from the PMA qPCR quantification a different pattern appears. For all samples but one (“*S. aureus* + *E. coli*”) nisin A treatment results in a decrease in bacterial number of all three bacteria (**Figure 21**). This could suggest an antimicrobial effect of nisin on both Gram-negative and Gram-positive bacteria, or it could indicate some form of interaction with the extracellular matrix components of the biofilm, that breaks down the rigid structure of a biofilm causing a bigger loss of bacteria in the wash step compared to the biofilm without treatment. The difference between the results of total biomass and bacterial count could also suggest that the staphylococci in the mixed species biofilms actually are killed but the structure of *E. coli* based biofilms differs from the other by keeping the dead staphylococci lodged in the biofilm matrix. As earlier stated nisin has greater effect on Gram-positive bacteria, since they cannot penetrate the outer membrane barriers of Gram-negative bacteria. This is in accordance with our findings. However, studies have shown that combinations of nisin with agents that destabilize the outer membrane of Gram-negative bacteria have been effective.^{61–63}

Slow growing bacteria in biofilm

The slow growth rate of biofilm bacteria seems to be a paramount obstacle for conventional antibiotics and it could be an issue for some AMPs as well. AMPs have multiple antimicrobial mechanisms and some of these are not independent on close bacterial interactions or normal growth rate of the affected bacteria, but none the less, differences between antimicrobial and anti-biofilm activity of the AMPs studied here are obvious. This is illustrated in the large differences between MIC values and biofilm eradicating concentrations of all the antimicrobial agents applied in this thesis. The superior biofilm eradicating effect of nisin A is probably contributed by its multiple modes of bacterial interactions rendering bacteria less resilient. Nisin A shows varying effects on different combinations of bacteria, but quite substantial decreases are seen in bacterial numbers; more than a 10-fold decrease in some cases (**Figure 21**). However, no results show complete removal of biofilm by nisin A even at the relatively high concentration utilized (64 µg/ml). It seems like all the different modes of actions of nisin are necessary to exert its full effect, and perhaps some of these actions are inhibited by the slow growth rate of bacteria in biofilms. This could certainly be the case for the

interaction between nisin and lipid II which inhibits biosynthesis of the cell wall as biosynthesis is halted in the dormant slow growing bacteria in the inner compartments of biofilms.

Method optimisation – Biofilm eradication assay

As the work of this thesis unfolded and, experience with different assay methods increased, it resulted in optimization of some of the methods utilised. As a result of this, a couple of remarks on the advantages and disadvantages of the different methods are discussed below.

Biofilm eradication measured by crystal violet staining

Regarding the biofilm eradication assay in general, rather large SD values were observed. It was evident already during the assay that especially the washing steps resulted in inconsistencies between replicate wells. This may be a result of the final washing procedure in the microtiter dish biofilm formation protocol⁴⁸ that warries from the procedure that other researchers at Roskilde University use. They use multi-well pipettes for every wash step, where the protocol by O'Tool instruct the use of washing trays where the microtiter plate is submerged under water in the final washing step where excess crystal violet stain that has not bound to biofilm is removed. There were also visually apparent differences in the amount of biofilm produced by the different species of bacteria. *S. aureus* formed markedly more biofilm than *S. epidermidis* and *E. coli*. This, and differences in their adherence abilities might affect the biofilms ability to endure washing steps. Examples of the effect of different wash steps are shown in **Figure 8** and **Figure 9**. **Figure 8 A** illustrates wells in triplicates after biofilm formation and 24 h treatment where media with planktonic bacteria has been removed. **Figure 8 B** illustrates the same wells after two washes with 150 µl PBS using multi-well pipettes. It is evident that a substantial amount of biofilm is removed by washing and already after this initial wash different amounts of biofilm remain in the triplicate wells. In **Figure 9** triplicate wells are illustrated after the final wash step where the microtiter plate is submerged under water to remove excess crystal violet. In rows C and F where *S. aureus* is seeded as the first (or only) bacteria we observe a stained biofilm that are washed away in a patchy/flaky manner. Again, contributing to inconsistent results from replicate wells. Also, the growth media chosen for the assay and the different bacteria's overall robustness will affect consistent results. An example of different SD values between similar biofilm eradication assays on two different bacterial species is also observed in figure 4 of this article by Field *et al.*⁵⁹ To conclude, the microtiter dish biofilm formation assay is the most widely used assay to measure biofilm eradication (Christensen *et al.*, 1995) but it seems that the assay requires a bit of practice and a rather high number of replicates to produce results with low deviation. Furthermore,

the crystal violet staining procedure will stain both live and dead bacteria together with extracellular matrix components resulting in total biomass results. For a more specific result of viable bacteria left in the biofilm after antimicrobial treatment the PMA qPCR method is utilized in this thesis.

Biofilm eradication determined by PMA qPCR

To investigate biofilm eradicating effects in different ways, and to elucidate the significance of biofilm structure in bacterial killing, quantification of viable bacteria in biofilms was assessed by PMA qPCR. Single and multi-species biofilms were formed and treated with antibiotics and nisin A nad GN-2. After treatment biofilms were detached from wells and treated with PMA to differentiate between viable and non-viable bacteria. DNA was extracted from each sample and quantified by qPCR.

DNA-extraction

To try and compensate for the inconsistent values described in the crystal violet staining procedure replicate wells from the biofilm forming assay were pooled before DNA-extraction and qPCR. DNA-extraction were conducted following manufactures protocol⁵⁰. In this procedure differences between bacterial species were also noted. For both staphylococci a less defined separation was achieved between the clear aqueous phase containing RNA and the interphase containing DNA. This could have resulted in inconsistent amounts of extracted DNA compared to samples only containing *E. coli* since complete removal of the RNA containing phase is essential for the purity of extracted DNA. This however, proved not to be an impediment as DNA content was measured and found consistent and sufficient for qPCR. Treatment with Lysostaphin was also tested but neither phase-separation or DNA yield was affected by this.

PMA treatment

PMA is an interacting dye that binds to DNA. By the utilisation of PMA discrimination between viable and non-viable cells was possible since only the DNA of non-viable bacteria are accessible to PMA due to compromised bacterial membranes. PMA binds the DNA of non-viable bacteria so this DNA cannot be amplified by qPCR leading to bacterial counts of only viable bacteria. PMA was tested on viable and heat-killed planktonic bacteria prior to biofilm eradication assays. Results of this test showed that PMA was able to bind DNA of bacteria with compromised bacterial membranes leading to significantly lower qPCR results for heat killed bacteria compared to viable bacteria.

Results of qPCR of viable, non-viable, and mixed planktonic *E. coli* is illustrated in **Figure 13**. Previous studies of PMA have showed similar results and proved that PMA is a better alternative than earlier applied chemicals like ethidium monoazide (EMA)^{65,66}. qPCR is a very sensitive method for amplification of even the smallest amounts of DNA and the PMA test do show ct-values of the heat killed *E. coli* sample, even though plating shows no viable bacteria in this sample (**Figure 14**). This shows that the binding of PMA to DNA of non-viable bacteria is not 100% effective, and should be kept in mind when assessing qPCR results of bacterial counts.

qPCR

Specific primers for each species were designed using Primer-BLAST from NCBI. Many different primers were tested to find primers that were specific for the individual species. As *S. aureus* and *S. epidermidis* are species from the same genera their genome exhibits a high degree of homology which can complicate the search for specific primers. In **Figure 15** and **Figure 16** the specificity of the two staphylococcal primers are illustrated. For the *S. epidermidis* 193 primer (**Figure 16**), almost complete specificity is observed with Ct values for *S. epidermidis* at 19 and for *S. aureus* above 35. The samples tested are DNA-extractions from samples containing planktonic bacteria of similar CFU/ml. The specificity of the *S. aureus* 149 primer is slightly less specific. **Figure 15** illustrates the different staphylococci samples measured with the *S. aureus* 149 primer and the *S. aureus* sample yields a low Ct of 15 showing high bacterial numbers but *S. epidermidis* yields a Ct of 25 which is not low enough to be outside the range of the *S. aureus* standard curve (**Figure 18**) This is probably the reason why bacterial counts for *S. aureus* are observed in samples that do not contain *S. aureus* e.g. the “*S. epidermidis*” sample and the “*S. epidermidis* + *E. coli*” sample in **Figure 20** and **Figure 21**. Consequently, the bacteria measured by the *S. aureus* 149 primer in these samples are probably *S. epidermidis*. Bacterial counts were calculated from Ct-values using standard curves from the different bacterial species. These were made from dilutions of planktonic samples with bacterial number identified by plating. Unfortunately, due to time constraints the biofilm eradication assay quantified by PMA qPCR was only done once which leaves no room for interpretation of the reproducibility of the assay. Also, no significant differences between treatments can be calculated due to this.

Wound healing properties of AMPs

Previous research suggest that the AMPs investigated in this thesis have both antimicrobial and immunomodulating mechanisms. To further investigate their immunomodulating abilities, AMPs were tested in an *ex-vivo* wound healing model using porcine skin. Different effects on wound healing was assessed for all four AMPs at day 0, 1 and 3 after wounding.

GN-2

The relatively new GN-2 is not as well studied as the other AMPs utilized in this thesis. Its antimicrobial activity has been studied as described earlier, but as of this moment no studies on immunomodulating effects of GN-2 has been found. In the wound healing model of this thesis GN-2 seems to aid in the wound healing progress on day 1 suggesting an effect on the early pro-inflammatory phase. Results show an increased epithelial ingrowth on day 1 in wounds treated with GN-2 compared to wounds without treatment (**Figure 23** and **Figure 29**). On day 3 on the other hand, GN-2 shows no difference in epithelial ingrowth and a thinner layer of newly formed epithelia together with low numbers of proliferating cells (**Figure 29**). The effect of GN-2 has clearly decreased on day 3 and the low number of proliferating cells could even suggest a toxic effect of GN-2 slowing down migration and overall metabolism of the porcine skin cells. These findings are however not completely unexpected as the toxicity of GN-2 peptide have previously been studied by Godballe et al. It was found by MTT toxicity assay on HeLa cells that a concentration of 47 µg/ml of GN-2 was sufficient to reduce metabolic activity by 50% (IC₅₀).³⁷ In the study by Godballe et al. HeLa cells were exposed to GN-2 for 1 h only. In the wound healing model of this thesis GN-2 containing media (64µg/ml) was added to the wounds every 24 h for the three days of the experiment. Still, the negative results on wound healing was not observed until day 3. This might suggest that lower concentrations of GN-2 or only one-time administration of peptide could have eluded the toxic effects of long-term GN-2 exposure. It should also be mentioned that the HeLa cells used to assess toxicity by Godballe et al. are immortal cells derived from tumors of cervical cancer and cancer cells are known to be negatively charged making them a potential target of the antimicrobial activities of the cationic peptide GN-2 discussed earlier.⁶⁷ Part of the high selectivity of GN-2 towards bacteria lies in the interaction with the negatively charged membrane of bacteria, and Godballe et al. did also show, that the hemolytic effect of GN-2 was markedly lower on human red blood cells (<10% hemolysis = 100 µg/ml GN-2).³⁷ More studies on different human cell lines would of course be necessary to exclude toxic effects of AMPs before therapeutic application is considered.

Nisin A

As earlier mentioned nisin is already used as a food preservative due to its antibacterial effect but the immunomodulating abilities of nisin has not been extensively studied. In a study by Pablo et al an effect on the adaptive immune system was observed. Nisin was incorporated in the diet of mice as the commercially available Nisaplin (a nisin preparation containing 2.5% nisin, 77.5% NaCl and non-fat dried milk) ⁶⁸ and administered for up to 100 days. An increase in T-lymphocytes and a decrease in B-lymphocytes were observed after short-term administration and an increase in the macrophage/monocyte fraction in peripheral blood was also increased. ⁶⁹ These findings demonstrate that nisin can have immunomodulating effects but the adaptive immune responses of nisin are not possible to assess in the short-term *ex-vivo* wound healing model of thesis. Kindrachuk et al studied the immunomodulating effects of nisin Z and found effects on both the innate and the adaptive immune system. Nisin Z is another naturally occurring variant of nisin closely resembling nisin A. Nisin Z differs from nisin A by a single amino acid residue at position 27, asparagine instead of histidine⁷⁰. Chemokines MPC-1, IL-8 and Gro- α was increased and TNF- α was decreased in response to bacterial LPS in peripheral blood mononuclear cells. ³⁹ The increase of chemokines like these will attract immune cells like neutrophils and macrophages to the injury site and combat infection by pathogens. Also, a decrease in TNF-a can promote healing by downregulating the inflammatory response. These results are in accordance with the findings of this thesis. On day 1 a significant increase in epithelial ingrowth is observed in wounds treated with nisin A compared to wounds without treatment (Figure 29) indicating that nisin A affects the initial phases of wound healing and increases migration of epithelial cells at this stage. On day three we do not observe a superior wound healing compared to the control as no increase in epithelial depth or in number of proliferating cells is apparent (Figure 29). This confirms that the effect of nisin A is most evident in the very early phases of wound healing. The wound healing model used in this thesis is not infected by bacteria or induced with LPS to simulate an infection by pathogens. Had this been applied, a stronger effect of nisin A could possibly be observed as the combination of antimicrobial and immunomodulating effects could be effectuated.

Substance P

SP is a neuropeptide found in the CNS and in numerous peripheral tissues. As a neuropeptide, SP has been investigated in numeral neurologic diseases and in relation to its role in the CNS but the peptide has also been found in the gastrointestinal tract and in skin where its effect on wound healing has

been studied^{43,71,72}. Some immunomodulatory effects of SP have been investigated but the comprehensive effects on wound healing are intricate and still not fully elucidated. Vang Mouritzen et al. have studied the effect on migration of human keratinocytes in a scratch assay and found that SP has a significant effect on wound closure⁷². SP additionally increased angiogenesis and mRNA expression of the pro-inflammatory cytokine IL-6 proving a significant role of SP in the complex orchestration that wound healing is⁷². Pro-inflammatory cytokines are important in the first stages of wound healing where the attraction of leukocytes and phagocytic cells are needed to combat pathogens. In later phases a shift to anti-inflammatory conditions are needed to progress onto proliferation and tissue remodelling. Failure to progress from a pro-inflammatory to anti-inflammatory state will result in chronic wounds which is the main problem of DFU⁷³. From the employed *ex-vivo* wound healing model no significant results were found for SP treatment on porcine skin wounds, but a tendency towards increased proliferation is notable (**Figure 29**). The number of cells identified by immunohistochemical staining with ki67 antibody is slightly increased on day three in the newly formed epithelia of SP treated wounds compared to wounds with no treatment. This is listed in **Table 7** and seen in **Figure 29**. An increase of proliferation in epithelial cells by topical SP treatment is also found by Jain and da Silva^{74,75}. A deeper investigation of cytokine expression and angiogenesis has not been performed in this study but this would give a more detailed picture of the specific effects of SP on the different days of wound healing. Also, prolonging the experiment more than three days would make it possible to assess later stages of wound healing.

Decreased levels of SP is found in skin under hyperglycaemic conditions^{42,71,75}. This correlates with the hindered progression onto a healing and anti-inflammatory status of diabetic wounds. In this study, no significant differences are noticed between day 1 and 3 in the more physical parameters investigated (**Figure 29**). We do observe a newly formed epithelia layer covering the entire wound bed on day 3 in every wound (**Figure 24**), and this might not have been the result, had we tested the wound healing model under high glucose conditions. Due to time constraints this was not possible, but the effect of SP and the other peptides tested in this thesis could very well be different under hyperglycaemic conditions and this would be very interesting to test regarding the potential use of AMPs as therapeutic agents in the healing of DFU.

Neurotensin

NT, like SP, is a neuropeptide found predominantly in the CNS but also in different peripheral tissues like the skin. The role of NT is less studied as the peptide has been identified later than SP and other

neuropeptides like neuropeptide Y (NPY) and Calcitonin Gene Related Peptide^{42,76}. Da Silva et al. and others have recently studied wound healing effects of NT and found that NT contrary to SP seems to favour the anti-inflammatory phases of wound healing^{72,76}

NT was found to decrease pro-inflammatory cytokines IL-6 and TNF- α in a model where inflammation was imitated by the addition of LPS⁷⁶ but in another study IL-6 was significantly increased in a macrophage cell line treated with NT⁷⁷ and yet another study shows no effect on IL-6 expression in NT treated HaCat cells⁷². Contradicting results are found in more aspects of the immunomodulating effects of NT, also regarding the expression of NT under hyperglycaemic conditions where Moura et al. observe decreased levels of NT in skin and da Silva writes about increased levels of NT in delayed wounds.⁷⁶ NT has different ways of interactions using different receptors and several factors in the wound environment will affect the outcome of NT treatment as well. Cytokine expression and growth factors also acts in different ways under different time points of wound healing so a definite distinction between pro- and anti-inflammatory cytokines are not always applicable either⁷⁸. Furthermore, diverging results may also be anticipated as a result of different models applied in the study of wound healing. Still more research is needed to elucidate the comprehensive effects of NT in wound healing but in two studies on full thickness excisional wounds on mice NT has demonstrated a positive effect on wound healing showing downregulation of inflammation and faster wound closure.^{46,79} Due to the short duration of the wound healing experiment in this thesis the later phases of wound healing like tissue renewal and –remodeling cannot be examined. A high level of proliferating cells and a slight increase in the depth of newly formed epithelia is however notable at day three in the wounds treated with NT (**Figure 16 C**). This supports an effect of NT on migration of epithelial cells, but no increase in epithelial ingrowth is visible at day one, suggesting a later phase effect of NT in wound healing. A thicker epithelial layer is also observed already on day 3 in a mouse wound healing model by Moura, but only in diabetic mice.⁷⁹ This further demonstrates the enhanced effect of NT in diabetic skin. Another positive effect on wound healing that has been illustrated is increased angiogenesis⁷², another very important issue to address in the therapeutic application of NT in DFU treatment. In conclusion, NT have demonstrated positive effects on wound healing but other research suggests a different effect from SP favoring the later phases of wound healing. No significant differences between the two neuropeptides are observed in this study, but a difference might be visible in a hyperglycemic model or at a longer duration of the assay. The different results found by others could suggest that the time for potential administration of NT in DFU could be of great importance. If NT predominantly has an anti-inflammatory effect on

wound healing, the effect on non-healing wounds like DFU could be significant. Reducing inflammation and prompting the progression into later anti-inflammatory phases could aid in the healing of chronic infected wounds.

Method optimisation - Wound healing

The *ex-vivo* porcine skin wound healing model applied in this thesis was a foray into uncharted territory. No experience with models using freshly harvested skin has been attempted in this research group and consequently the execution and optimisation of this model turned into a minor study of its own. The patented model by Vielhaber et al (Patent: EP 2019316 A2) was applied and adapted. Use of porcine skin as a substitute for human skin was chosen because of its high resemblance and the accessibility as discussed earlier. Difficulties in achieving consistent wounds was the main problem and led to the testing and invention of several different instruments. Pictures of these instruments are depicted in **Figure 30** in Appendix. A 2 mm diameter biopsy punch was implemented in the final wound healing model and illustrations of these wounds after different treatments are seen in **Figure 22**, **Figure 23**, and **Figure 24**. It is evident that wound depth still varies a bit, but replicate samples should compensate for this. More than three replicates could be applied for greater statistical power. The time points for observation was selected to time 0 (directly after wounding), day 1, and day 3. A complete coverage of wound surface with newly formed epithelia was observed in every wound at day 3. Therefore, to be able to detect differences between treatments samples were also taken at day 1, and a time point even earlier, maybe 8-16 h after wounding, could maybe have contributed with even more information. To assess later phases of wound healing a longer duration would have been preferred. However, tests were made to estimate the possible durability of the test and at day 8 no proliferating cells were observed (illustrated by ki67 staining) demonstrating poor viability of skin cells at this point (Appendix, **Figure 31**). Other studies utilising similar *ex-vivo* wound healing models have showed viability of up to 14 days post wounding^{80,81}, but it was not possible to maintain viability here and also infections were observed in some wounds when exceeding day 5.

Immunohistochemical staining with ki67 antibody was made at Copenhagen University. The antibody used was directed against human antigen ki67 but it proved that the same antigen is present in porcine skin. Antibodies against NT and SP was also tested, but these showed only unspecific staining (Appendix, **Figure 32**).

Furthermore, testing under hyperglycaemic conditions and simulated inflammation by addition of LPS was planned, to mimic the circumstances of DFU, but due to time constraints this was not possible.

AMPs as therapeutic agents

Increasing prevalence of bacteria resistant to conventional antibiotics is becoming more and more evident and the need for novel treatment against bacterial infections are much needed. AMPs have come of great interest amongst researchers in this field because of their broad spectrum of antimicrobial activity. Other things adding to the prospects of AMPs are their natural occurrence amongst several species as elements of host defence suggesting low toxicity and providing easy availability. AMPs exert their antimicrobial actions by multiple mechanisms also making resistance development less likely. Observations of immunomodulating abilities like the once observed in this study now adds even more possibilities to the potential therapeutic applications for AMPs. Conversely, immunomodulating effects can also have disadvantageous effects, and must be thoroughly investigated before therapeutic application can be considered. For example, the toxic effects of GN-2 in this wound healing model course for concern and must be further investigated.

Generally, it seems there are many desirable actions of AMPs both regarding direct antimicrobial killing and immunomodulating abilities. Success in combining these different mechanisms of wound healing and eliminate toxic effect could lead to a possible treatment of chronic wounds like DFU. A combination of antimicrobial and immunomodulating peptides could further potentiate a possible therapeutic application, but further studies on synergistic or antagonistic effects would then be necessary too. Vang Moureitzen et al. shows antagonistic effects of NT and SP when used in combination⁷². Results from the wound healing model supports different healing mechanisms of the different peptides, and the different phases of wound healing being affected by different peptides could also indicate that time of administration should vary in a possible treatment strategy.

Other aspects like costs and large scale production are things to be considered as well along with administration methods. Since peptides are degraded by peptidases in body fluids relatively fast⁸² alternatives to topical or oral administration could be considered. Moura et al has had positive results with the use of wound dressings combined with NT^{46,79} and Heunis et al. has also applied nisin-eluting nanofiber wounds dressings to treat *S. aureus* infected wounds⁴¹

Conclusion

The aim of this thesis was to investigate wound healing properties of four antimicrobial peptides (AMPs) in the search for alternatives to antibiotic treatment of DFU. Different assays were applied to assess immunomodulating and biofilm eradicating properties of GN-2, nisin A, NT, and SP.

Results of biofilm eradication assays show minor effects of GN-2 on biofilm eradication. Better results were observed by nisin A which were able to reduce bacterial numbers in almost every type of biofilms, single- or multi-species. Immunomodulating effects of both GN-2 and nisin A, as an increase on epithelial cell migration, were observed on day 1 in an *ex-vivo* wound healing model using porcine skin. NT and SP showed immunomodulating effects on day 3 where, especially NT, showed increased numbers of proliferating cells. In conclusion, different interesting effects on wound healing was observed by the four investigated AMPs adding to the elucidation needed for the potential use of AMPs as therapeutic agents.

References

1. International Diabetes Federation. *IDF DIABETES ATLAS - Eighth edition 2017*. (2017).
2. Katsilambros, N., Dounis, E., Makrilakis, K., Tentolouris, N. & Tsapogas, P. *Atlas of the Diabetic Foot. Atlas of the Diabetic Foot* (Wiley-Blackwell, 2011). doi:10.1002/9781444317589
3. Bjarnsholt, T. The role of bacterial biofilms in chronic infections. *APMIS. Suppl.* **136**, 1–51 (2013).
4. Von Nussbaum, F., Brands, M., Hinzen, B., Weigand, S. & Häbich, D. Antibacterial natural products in medicinal chemistry - Exodus or revival? *Angewandte Chemie - International Edition* **45**, 5072–5129 (2006).
5. Martini et al. *Human Anatomy, Eighth Edition*. (Pearson, 2015).
6. Porth, C. M. *Essentials of Pathophysiology. Essentials of pathophysiology 3rd Ed.* (2011).
7. Singer, A. J. & Clark, R. A. F. Cutaneous Wound Healing. *N. Engl. J. Med.* (2008).
8. Bowler, P. G. Wound pathophysiology, infection and therapeutic options. *Ann. Med.* **34**, 419–427 (2002).
9. Meurens, F., Summerfield, A., Nauwynck, H., Saif, L. & Gerdtts, V. The pig: A model for human infectious diseases. *Trends Microbiol.* **20**, 50–57 (2012).
10. Summerfield, A., Meurens, F. & Ricklin, M. E. The immunology of the porcine skin and its value as a model for human skin. *Mol. Immunol.* **66**, 14–21 (2015).
11. Debeer, S. et al. Comparative histology and immunohistochemistry of porcine versus human skin. *Eur. J. Dermatology* **23**, 456–466 (2013).
12. Ranamukhaarachchi, S. A. et al. A micromechanical comparison of human and porcine skin before and after preservation by freezing for medical device development. *Sci. Rep.* **6**, 1–9 (2016).
13. Wester, R. C., Melendres, J., Sedik, L., Maibach, H. & Riviere, J. E. Percutaneous absorption of salicylic acid, theophylline, 2, 4-dimethylamine, diethyl hexyl phthalic acid, and p-aminobenzoic acid in the isolated perfused porcine skin flap compared to man in vivo. *Toxicol. Appl. Pharmacol.* **151**, 159–165 (1998).
14. Perim, M. C. et al. Aerobic bacterial profile and antibiotic resistance in patients with diabetic foot infections. *Rev. Soc. Bras. Med. Trop.* **48**, 546–554 (2015).
15. Costerton, J. W., Geesey, G. G. & Cheng, K. J. How bacteria stick. *Sci. Am.* **238**, 86–95 (1978).
16. Leeuwenhoek, A. Microscopical observations about animals in the scurf of the teeth. *Philos Trans.* **14**, 568–574 (1684).
17. Beloin, C., Roux, A. & Ghigo, J. M. Escherichia coli biofilms. *Curr. Top. Microbiol. Immunol.* **322**, 249–89 (2008).
18. Otto, M. Staphylococcal Biofilms. *Curr Top Microbiol Immunol.* **31**, 1713–1723 (2013).
19. Liu, W. et al. Interspecific bacterial interactions are reflected in multispecies biofilm spatial

- organization. *Front. Microbiol.* **7**, 1–8 (2016).
20. Ehrlich, P. & Hata, S. *Die experimentelle Chemotherapie der Spirillosen.* (Springer Berlin Heidelberg, 1910). doi:10.1007/978-3-642-64926-4
 21. Mahoney, J. F., Arnold, R. C. & Harris, A. Penicillin Treatment of Early Syphilis-A Preliminary Report. *Am. J. Public Health Nations. Health* **33**, 1387–91 (1943).
 22. Fischbach, M. A. & Walsh, C. T. Antibiotics For Emerging Pathogens Michael. *Science (80-.)*. **325**, 1089–1093 (2009).
 23. Wright, G. D. Q&A: Antibiotic resistance: Where does it come from and what can we do about it? *BMC Biol.* **8**, (2010).
 24. World Health Organization. WHO Model List of Essential Medicines. *Essent. Med. Heal. Prod.* 1–39 (2017). doi:10.1016/S1473-3099(14)70780-7
 25. Kohanski, M. A., Dwyer, D. J. & Collins, J. J. How antibiotics kill bacteria : from targets to networks. *Nat Rev Microbiol* **8**, 423–435 (2010).
 26. Waller, D. G., Sampson, A. P., Renwick, A. G. & Hillier, K. *Medical Pharmacology and Therapeutics* , Fourth Edition. 323–334 (2014).
 27. Howden, B. P., Davies, J. K., Johnson, P. D. R., Stinear, T. P. & Grayson, M. L. Reduced vancomycin susceptibility in *Staphylococcus aureus*, including vancomycin-intermediate and heterogeneous vancomycin-intermediate strains: Resistance mechanisms, laboratory detection, and clinical implications. *Clin. Microbiol. Rev.* **23**, 99–139 (2010).
 28. Shahbaz, K. Cephalosporins : pharmacology and chemistry. **4**, 234–238 (2017).
 29. Harada, S. New Cephalosporins. *J. Chromatogr. Libr.* **43**, 233–257 (1989).
 30. Immunopedia.org. Treatment of Mycobacterium tuberculosis . 1s t line antibiotic drugs. *Immunopedia.org*
 31. Wehrli, W. Rifampin : Mechanisms of Action and Resistance Author (s): Walter Wehrli Source : *Reviews of Infectious Diseases* , Vol . 5 , Supplement 3 . The Use of Rifampin in the Treatment of Nontuberculous Infections (Jul . - Aug . , 1983), pp . S407-S411 Publish. *Rev. Infect. Dis.* **5**, S407–S411 (1983).
 32. EUCAST. Eucast. Available at: <https://mic.eucast.org/Eucast2/>. (Accessed: 19th May 2018)
 33. Mota-Meira, M., LaPointe, G., Lacroix, C. & Lavoie, M. C. MICs of mutacin B-Ny266, nisin A, vancomycin, and oxacillin against bacterial pathogens. *Antimicrob. Agents Chemother.* **44**, 24–29 (2000).
 34. Fjell, C. D., Jenssen, H., Cheung, W. A., Hancock, R. E. W. & Cherkasov, A. Optimization of Antibacterial Peptides by Genetic Algorithms and Cheminformatics. *Chem. Biol. Drug Des.* **77**, 48–56 (2011).
 35. Reddy, K. V. R., Yedery, R. D. & Aranha, C. Antimicrobial peptides: Premises and promises.

- International Journal of Antimicrobial Agents* **24**, 536–547 (2004).
36. Nagao, J. Properties and Applications of Lantibiotics, a Class of Bacteriocins Produced by Gram-positive Bacteria. *J. Oral Biosci.* **51**, 158–164 (2009).
 37. Godballe, T., Mojsoska, B., Nielsen, H. M. & Jenssen, H. Antimicrobial activity of GN peptides and their mode of action. *Biopolymers* **106**, 172–183 (2016).
 38. Begde, D. *et al.* Immunomodulatory efficacy of nisin-a bacterial lantibiotic peptide. *J. Pept. Sci.* **17**, 438–444 (2011).
 39. Kindrachuk, J. *et al.* Manipulation of innate immunity by a bacterial secreted peptide: Lantibiotic nisin Z is selectively immunomodulatory. *Innate Immun.* **19**, 315–327 (2013).
 40. van Staden, A. D. P., Heunis, T., Smith, C., Deane, S. & Dicks, L. M. T. Efficacy of lantibiotic treatment of *Staphylococcus aureus*-induced skin infections, monitored by *in vivo* bioluminescent imaging. *Antimicrob. Agents Chemother.* **60**, 3948–3955 (2016).
 41. Heunis, T. D. J., Smith, C. & Dicks, L. M. T. Evaluation of a nisin-eluting nanofiber scaffold to treat staphylococcus aureus-induced skin infections in mice. *Antimicrob. Agents Chemother.* **57**, 3928–3935 (2013).
 42. Leena Pradhan, P., Christoph Nabzdyk, B., Nicholas D Andersen, M., Frank W LoGerfo, M. & Aristidis Veves, MD, Ds. Inflammation and Neuropeptides: The Connection in Diabetic Wound Healing. *Expert Rev Mol Med* **11: e2. do**, (2013).
 43. Delgado, A. v., McMANuS, A. T. & CHAMBERS, J. P. Exogenous Administration of Substance P Enhances Wound Healing in a Novel Skin-Injury Model. *Soc. Exp. Biol. Med.* (2005).
 44. Park, J. H., Kim, S., Hong, H. S. & Son, Y. Substance P promotes diabetic wound healing by modulating inflammation and restoring cellular activity of mesenchymal stem cells. *Wound Repair Regen.* **24**, 337–348 (2016).
 45. Antezana, M. A. *et al.* Neutral endopeptidase activity is increased in the skin of subjects with diabetic ulcers. *J. Invest. Dermatol.* **119**, 1400–1404 (2002).
 46. Moura, L. I. F. *et al.* Neurotensin-loaded collagen dressings reduce inflammation and improve wound healing in diabetic mice. *Biochim. Biophys. Acta - Mol. Basis Dis.* **1842**, 32–43 (2014).
 47. Moura, L. I., Cruz, M. T. & Carvalho, E. The effect of neurotensin in human keratinocytes - implication on impaired wound healing in diabetes. *Exp. Biol. Med.* **239**, 6–12 (2014).
 48. O’Toole, G. A. Microtiter Dish Biofilm Formation Assay. *J. Vis. Exp.* 10–11 (2011).
doi:10.3791/2437
 49. Luo, Y. *et al.* Peptoid Efficacy against Polymicrobial Biofilms Determined by Using Propidium Monoazide-Modified Quantitative PCR. *ChemBioChem* **18**, 111–118 (2017).
 50. Sigma-Aldrich. TRI Reagent® - TECHNICAL BULLETIN.
 51. Johani, K. *et al.* Microscopy visualisation confirms multi-species biofilms are ubiquitous in diabetic

- foot ulcers. *Int. Wound J.* **14**, 1160–1169 (2017).
52. Okuda, K. I. *et al.* Effects of bacteriocins on methicillin-resistant *Staphylococcus aureus* biofilm. *Antimicrob. Agents Chemother.* **57**, 5572–5579 (2013).
53. Ashby, M. J., Neale, J. E., Knott, S. J. & Critchley, I. A. Effect of antibiotics on non-growing planktonic cells and biofilms of *Escherichia coli*. *J. Antimicrob. Chemother.* **33**, 443–452 (1994).
54. Brown, M. R. W., Allison, D. G. & Gilbert, P. Resistance of bacterial biofilms to antibiotics: a growth-related effect? *J. Antimicrob. Chemother.* 777–783 (1988).
doi:<https://doi.org/10.1093/jac/22.6.777>
55. Saporito, P., Jenssen, H. & Olesen, A. L. RESEARCH ARTICLE LL - 37 fragments have antimicrobial activity against *Staphylococcus epidermidis* biofilms and wound healing potential in HaCaT cell line. 1–12 (2018). doi:10.1002/psc.3080
56. Godballe, T. & Jenssen, H. Mode of action studies on synthetic antimicrobial peptide - Master thesis. *Department Sci. Syst. Model.* (2013).
57. Saporito, P. *PhD Thesis Synthesis and activity of antimicrobial peptides.* (2018).
58. Zacharof, M. P. & Lovitt, R. W. Bacteriocins Produced by Lactic Acid Bacteria A Review Article Bacteriocins Produced by Lactic Acid Bacteria A Review Article. *APCBEE Procedia* **2**, 50–56 (2012).
59. Field, D., O'Connor, R., Cotter, P. D., Ross, R. P. & Hill, C. In vitro activities of nisin and nisin derivatives alone and in combination with antibiotics against *Staphylococcus* biofilms. *Front. Microbiol.* **7**, 1–11 (2016).
60. Punyaappa-path, S. & Phumkhachorn, P. Nisin: production and mechanism of antimicrobial action. *Int. J. Curr. Res. Rev.* **7**, 47–53 (2015).
61. Lee, J. I., Lee, H. J. & Lee, M. H. Synergistic effect of nisin and heat treatment on the growth of *Escherichia coli* O157:H7. *J Food Prot* **65**, 408–410 (2002).
62. Schved, F., Henis, Y. & Juven, B. J. Response of spheroplasts and chelator-permeabilized cells of Gram-negative bacteria to the action of the bacteriocins pediocin SJ-1 and nisin. *Int. J. Food Microbiol.* **21**, 305–314 (1994).
63. Masschalck, B. Inactivation of high pressure resistant *Escherichia coli* by lysozyme and nisin under high pressure. *Innov. Food Sci. Emerg. Technol.* **1**, 39–47 (2000).
64. Christensen, G. D., Baldassarri, L. & Andrew Simpson, W. [38] Methods for studying microbial colonization of plastics. *Methods Enzymol.* **253**, 477–500 (1995).
65. Nocker, A., Cheung, C. Y. & Camper, A. K. Comparison of propidium monoazide with ethidium monoazide for differentiation of live vs. dead bacteria by selective removal of DNA from dead cells. *J. Microbiol. Methods* **67**, 310–320 (2006).
66. Lee, J. L. & Levin, R. E. A comparative study of the ability of EMA and PMA to distinguish viable

- from heat killed mixed bacterial flora from fish fillets. *J. Microbiol. Methods* **76**, 93–96 (2009).
67. Slaninová, J. *et al.* Toxicity study of antimicrobial peptides from wild bee venom and their analogs toward mammalian normal and cancer cells. *Peptides* **33**, 18–26 (2012).
68. Cotter, P. D., Hill, C. & Ross, R. P. BACTERIOCINS: DEVELOPING INNATE IMMUNITY FOR FOOD Paul. *Food Microbiol.* **3**, (2005).
69. De Pablo, M. A. *et al.* Evaluation of immunomodulatory effects of nisin-containing diets on mice. *FEMS Immunol. Med. Microbiol.* **24**, 35–42 (1999).
70. MULDER, J. W. M., BOERTGTTER, I. J., ROLLEMA, H. S., SIEZEN, R. J. & VOS, W. M. de. Mulders - Identification and characterization of the lantibiotic nisin 2, a natural nisin variant.pdf. *Eur. J. Biochem* **201**, 581–584 (1991).
71. Scott, J. R. *et al.* Topical substance P increases inflammatory cell density in genetically diabetic murine wounds. *Wound Repair Regen.* **16**, 529–533 (2008).
72. Vang Mouritzen, M. *et al.* Neurotensin , Substance P , and Insulin increases in vitro wound healing. *J. Pept. Sci.* (2018).
73. Landén, N. X., Li, D. & Stähle, M. Transition from inflammation to proliferation: a critical step during wound healing. *Cell. Mol. Life Sci.* **73**, 3861–3885 (2016).
74. Jain, M., Logerfo, F. W., Guthrie, P. & Pradhan, L. Effect of hyperglycemia and neuropeptides on interleukin-8 expression and angiogenesis in dermal microvascular endothelial cells. *J. Vasc. Surg.* **53**, 1654–1660.e2 (2011).
75. da Silva, L., Carvalho, E. & Cruz, M. T. Role of neuropeptides in skin inflammation and its involvement in diabetic wound healing. *Expert Opin. Biol. Ther.* **10**, 1427–1439 (2010).
76. da Silva, L., Neves, B. M., Moura, L., Cruz, M. T. & Carvalho, E. Neurotensin downregulates the pro-inflammatory properties of skin dendritic cells and increases epidermal growth factor expression. *Biochim. Biophys. Acta* **1813**, 1863–1871 (2011).
77. Moura, L. I. F. *et al.* Neurotensin modulates the migratory and inflammatory response of macrophages under hyperglycemic conditions. *Biomed Res. Int.* **2013**, 941764 (2013).
78. Cavaillon, J. PRO- versus ANTI-INFLAMMATORY CYTOKINES : *Cell. Mol. Biol.* (2014).
79. Moura, L. I. F. *et al.* Chitosan-based dressings loaded with neurotensin - An efficient strategy to improve early diabetic wound healing. *Acta Biomater.* **10**, 843–857 (2014).
80. Krüger, C. Der Einfluss von Östrogen auf die Wundheilung im porcinen System. 1–105 (2014).
81. Mendoza-Garcia, J., Sebastian, A., Alonso-Rasgado, T. & Bayat, A. Optimization of an ex vivo wound healing model in the adult human skin: Functional evaluation using photodynamic therapy. *Wound Repair Regen.* **23**, 685–702 (2015).
82. Starr, C. G. & Wimley, W. C. Antimicrobial peptides are degraded by the cytosolic proteases of human erythrocytes. *Biochim. Biophys. Acta - Biomembr.* **1859**, 2319–2326 (2017).

83. Mcstrother. File:Vancomycin resistance.svg - Wikimedia Commons. Available at: https://commons.wikimedia.org/wiki/File:Vancomycin_resistance.svg. (Accessed: 30th May 2018)
84. Sherrard, L. J., Tunney, M. M. & Elborn, J. S. Antimicrobial resistance in the respiratory microbiota of people with cystic fibrosis. *Lancet* **384**, 703–713 (2014).

Appendix



Figure 30 Pictures of different instruments tested for infliction of wounds to the porcine skin of the utilised ex-vivo wound healing model.

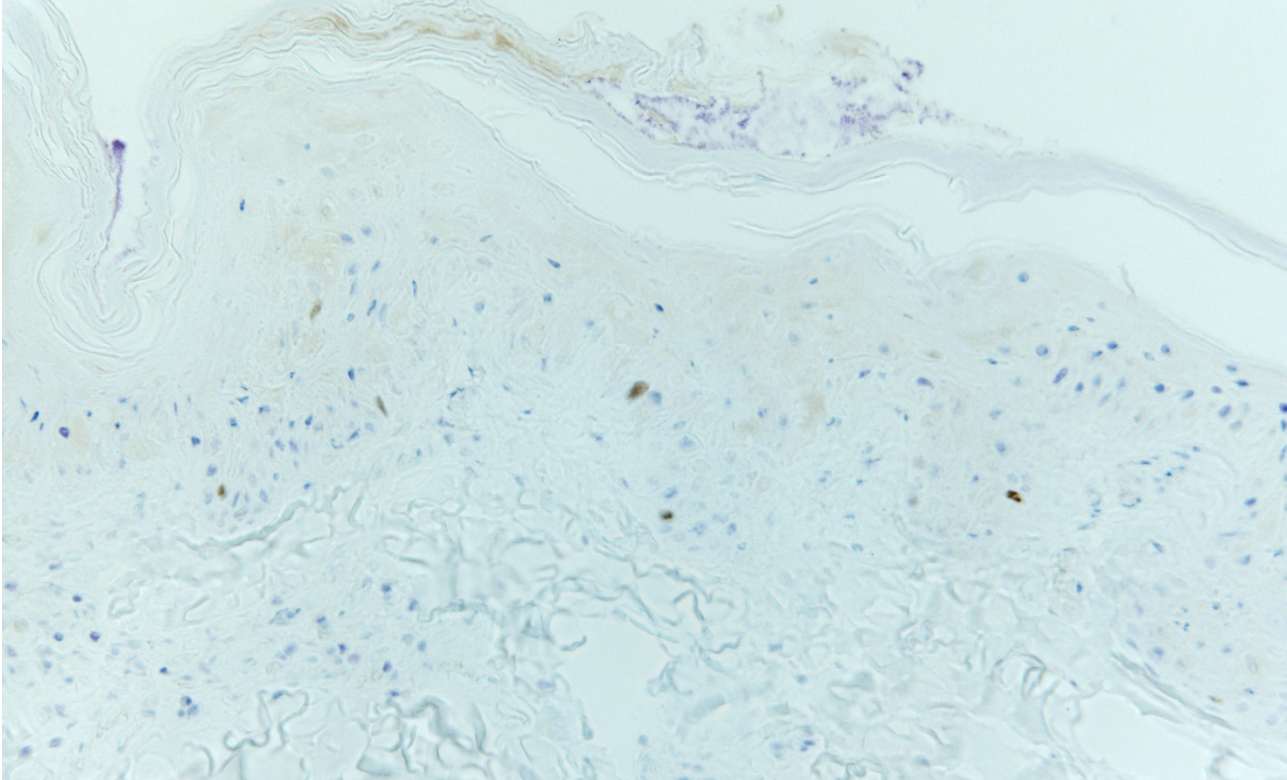


Figure 31 Porcine skin 8 days after excision. Immunohistochemical staining with ki67 showed no proliferating cells. 10x magnification.

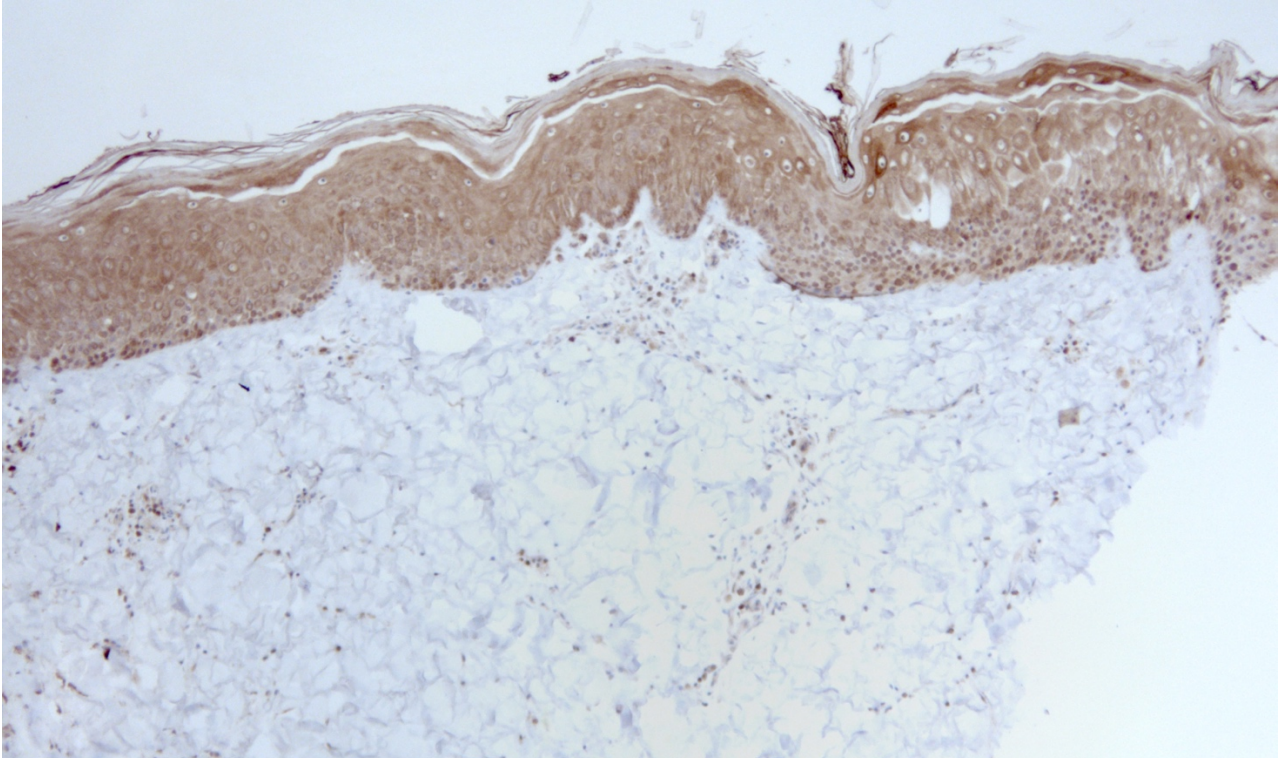


Figure 32 Immunohistochemical staining with SP antibody showed only unspecific binding in the entire epithelium. 5x magnification.